Modelling storm-induced beach/dune evolution: Sefton coast, Liverpool Bay, UK

Pushpa Dissanayake (Corresponding author)

Energy and Environment Research Group, College of Engineering, Swansea University, Singleton Park, Swansea, SA2 8PP, UK

++44(0) 1792 295540

++44(0) 1792 295676

p.k.dissanayake@swansea.ac.uk

Jennifer Brown

National Oceanographic Centre, Joseph Proudman Building, 6 Brownlow Street, Liverpool, L3 5DA, UK

jebro@pol.ac.uk

Harshinie Karunarathna

Energy and Environment Research, College of Engineering, Swansea University, Singleton Park, Swansea, SA2 8PP, UK

h.u.karunarathna@swansea.ac.uk

Abstract

Storm-induced dune evolution on a sandy coastal system is investigated using a nested modelling approach applied to the Sefton coast, Liverpool Bay, UK. Real-time offshore water levels and waves were used as model boundary forcings. A Delft3D coarse grid setup is used to simulate time and space varying sea surface elevations on which offshore waves are transformed (by applying the SWAN model) to establish the wave boundary for the high resolution morphological model (XBeach). Statistical comparisons between model predicted and measured post-storm profiles at a number of locations along the coast suggest that XBeach successfully captures storm-induced beach change along the Sefton coast. Predicted bed evolution of the beach/dune system shows alternate erosion and sedimentation areas in the nearshore. Strong bed level changes are found at the northern part of the Sefton coast when north-westerly (NW) extreme waves and winds coincide with spring-high tide. Morphological changes in the southern part are significantly lower than that in the north as a result of NW wave dissipation on the shoals located to the north of the Crosby channel, which creates low wave actions in that area. In addition, erosion of the dune foot is observed at some locations along the beach. Temporal simulation of beach/dune evolution as a result of variable forcing conditions during storms provides useful insight into the morphodynamic processes of beach/dune systems during storms (using Sefton as an example), which is very useful for developing coastal management strategies over the existing conceptual tools.

Key words: *real-time boundary forcing, dune erosion, profile evolution, XBeach, Sefton coast, Liverpool Bay*

1. Introduction

Coastal dune systems provide natural defence against erosion and flooding. They also provide an important natural habitat to local flora and fauna (Carter, 1988). Development and existence of coastal dunes are mainly controlled by cross-shore sediment transport delivering sediment to the upper beach and then Aeolian transport reshaping deposited sand (Harley and Ciavola, 2013). It is generally found that winter storms cause steep cross-shore profiles by dune erosion and offshore sediment transport while calm, mild summer conditions system recovery results in a more gentle profile shape in most of the world's coastal systems (Callaghan et al., 2008). Severe storms in winter are responsible for non-recoverable erosion leading to dune breaching and then subsequent flooding of the hinterland areas.

There are four regimes of dune change during storm events depending on the water level and the upper limit (the 2% exceedance level, R2%) of wave run-up heights (Sallenger, 2000). They are: 1) the swash regime – the dune system remains untouched, 2) the collision regime – wave bores collide with the dune face, 3) the overwash regime – a fraction of the waves overtop the dune crest and 4) the inundation regime – the dune is completely submerged. Episodic slumping of the dune face occurs during the collision regime (Palmsten and Holman, 2012; Erikson et al., 2007; Vellinga, 1986). The dune crest height can be rapidly reduced during the overwash and inundation regimes because

sediment is transported both landwards and seawards from the dune (Donnelly et al., 2006).

Storm-induced dune erosion is one of the major concerns of coastal safety and sustainable development in the areas where frontal dune systems are present. In recent years, there is growing attention to investigate and understand the storm driven dune erosion processes in terms of numerical modelling approaches and statistical simulations (Pender and Karunarathna, 2013; Callaghan et al., 2008; McCall et al., 2010; Lindemer et al., 2010; Ranasinghe et al., 2011; Williams et al., 2011; Harley and Ciavola, 2013) due to possible changes in future storminess.

Numerical modelling approaches have been developed over the last years in order to predict more accurate and reliable dune evolution (Stive and Wind, 1986; Larson and Kraus, 1989; Roelvink and Stive, 1989; Bosboom et al., 2000; Larson et al., 2004; Roelvink et al., 2009). XBeach is one of the latest developments and an *off-the-shelf* model which is being continually improved by applications in different coastal environments around the world. This model has proven to be capable of predicting morphodynamic storm impacts of beach/dune systems in numerous case studies (Roelvink et al., 2009; McCall et al., 2010; Harley and Ciavola, 2013; Harley et al., 2011; Lindemer et al., 2010; Splinter and Palmsten, 2012; Williams et al., 2011). These studies motivated us to use and test the XBeach model to investigate storm driven beach/dune evolution in hyper-tidal conditions along the Sefton coast, Liverpool Bay, UK.

In previous research, different methods have been carried out in Liverpool Bay and specifically on the Sefton coast to hindcast and forecast wave climate, tidal-surge propagation and morphological evolution (Jones and Davies, 1998; Esteves et al., 2012; Brown et al., 2010a,b,c; Woodworth et al, 2007; Esteves et al., 2011; Wolf et al., 2011; Wolf and Woolf, 2006; Pye and Neal, 1994; Pye and Blott, 2008; Brown et al., 2012; Brown, 2010 and many others). Numerical models were mainly used to investigate the hydrodynamic characteristics (wave climate, tide, surges and their interactions leading to extreme events) under existing and future scenarios of sea level rise and climate change locally and also over the larger scale of the Irish Sea (Brown et al., 2012; Brown et al., 2010a,b,c; Wolf et al., 2011; Woodworth et al., 2007; Brown, 2010; Wolf and Woolf, 2006; Jones and Davies, 1998), to identify the importance of externally and locally generated conditions to Liverpool Bay. Although these results are not directly applicable to the Sefton coast, they provide potential offshore boundary conditions which can be used to model the local morphodynamics. Only a few studies discuss morphological evolution along the Sefton coast itself (Esteves et al., 2012; Williams et al., 2011; Esteves et al., 2011; Esteves et al., 2009; Halcrow, 2009; Pye and Neal, 1994; Pye and Blott, 2008) and they have mainly focused on historical data analysis implying the general patterns of morphological changes. Pye and Neal (1994) analysed the historical shoreline changes from 1845 to 1990 and found that middle reaches of the Sefton coast is eroding (~ 3 m/year) while northern and southern parts are accreting (~ 1 m/year). Decadal variation in dune erosion and accretion from 1958 to 2008 was investigated by Pye and Blott (2008) using a series of beach and dune surveys. This analysis shows that severe dune erosion occurs when storms generate positive surges on several successive tides.

Esteves et al (2012) have quantified water level, significant wave height and dune erosion on the Sefton coast during several historical storm events and developed linear relationships among them in order to establish a threshold condition for dune erosion. In their study, dune erosion was estimated using one-dimensional (1D) profile data and they emphasized that inclusion of alongshore variation in the beach/dune morphology (i.e. 2D approach) is important to investigate dune evolution during stormy conditions. The MICORE project (Ciavola and Jimenez, 2011; Williams et al., 2011) has specifically focused on the storm driven dune erosion and potential hinterland flooding on the Sefton coast. They adopted the XBeach model (in 1D and 2D) imposing time-invariant wave boundary conditions (i.e. single wave condition) over a tidal cycle in a localised model domain for each tested scenario. These boundary forcings imply a conservative approach compared with the real-time storm-driven forcings and thus could lead to overestimation of morphodynamic changes of the beach/dune system.

The objective of the present study is to investigate the spatial variability of the exchange of sediment between dune face and beach during a storm, and to examine the alongshore variability of sediment dynamics in determining the evolution of the Sefton beach/dune system at engineering timescales. Such information is vital in taking effective and sustainable coastal management decisions.

There are a number of coastal management practices on the Sefton beach/dune system implemented by the Sefton Metropolitan Borough Council to deal with nature conservation and land management, shoreline management, coastal defence and flood

risk, recreation, leisure and tourism (Houston, 2010; McAleavy; 2010). Success of these strategies depends on the understanding of how this complex beach/dune system interacts with coastal processes not only over the long-term, but also during storm conditions, with focus on the spatial and temporal variation of the resulting sediment fluxes and in turn the morphological changes. Application of numerical models is very efficient and effective in order to get such high resolution details of the beach/dune system. Previously, an event scale 1D early warning system for erosion has been developed for Formby Point (Souza et al., 2013). In this paper a 2D application of numerical models is used to identify the processes causing storm driven morphological change to support conceptual modelling based on beach monitoring that informs the local shoreline management plans. This research will therefore supplement the bi-annual beach surveys carried out by the Sefton Metropolitan Borough Council by providing detailed information of storm impacts at the individual event scale, in addition to the seasonal observations that capture the longer term beach and dune response.

In this study a nested modelling approach is used. A larger, coarse grid, 2D model domain is used to transform real-time offshore boundary forcings into the nearshore area. A high resolution, smaller domain, which represents the initial bed topography and in turn the resulting erosion and sedimentation patterns, is set up to investigate storm-induced dune evolution along the Sefton coast. Implementing real-time boundary forcing in the model allows more realistic storm induced interactions between the hydrodynamics and morphodynamic evolution.

196 This paper is structured as follows. Section 2 and 3 describe the study area and the
197 selected storm event respectively. Section 4 describes the modelling approach used to
198 obtain the results given in section 5. A discussion of the overall findings is present in
199 section 6 while section 7 provides conclusions.
200
201
202
203

204 ## 2. Study area - Sefton coast

205

206 The Sefton coast is located between the Mersey estuary (to the south) and the Ribble
207 estuary (to the north) in Liverpool Bay. It is an approximately 36 km long convex shape
208 coastal stretch (Figure 1a) (Williams et al., 2011; Brown et al., 2010a,b; Pye and Blott,
209 2008; Plater and Grenville, 2010). The Sefton coastal system consists of natural
210 beaches/dunes which have high recreational and nature conservational value, engineered
211 beaches protected by seawalls, groynes and revetments and, rubble beaches covered with
212 building material debris and rock armours (Figure 1b). The dunes within the system
213 extend about 4 km inland, reach about 30 m ODN in height at some locations and
214 represents around 20% of the entire UK dune population (Souza et al., 2013; Esteves et
215 al., 2012; Williams et al., 2011; Pye and Blott, 2010; Esteves et al., 2009). These dunes
216 form an effective natural coastal flood defence for the local urban areas, high grade
217 agricultural lands and a significant number of conservational areas of national and
218 international interest. It also consists of extremely high biodiversity that includes rare and

endangered species (Edmondson, 2010; White, 2010; Smith, 2010). Growth and existence of these highly valued natural systems depends on the sustainability of the beach/dune system, which is currently under threat due to erosion and nearby manmade developments.

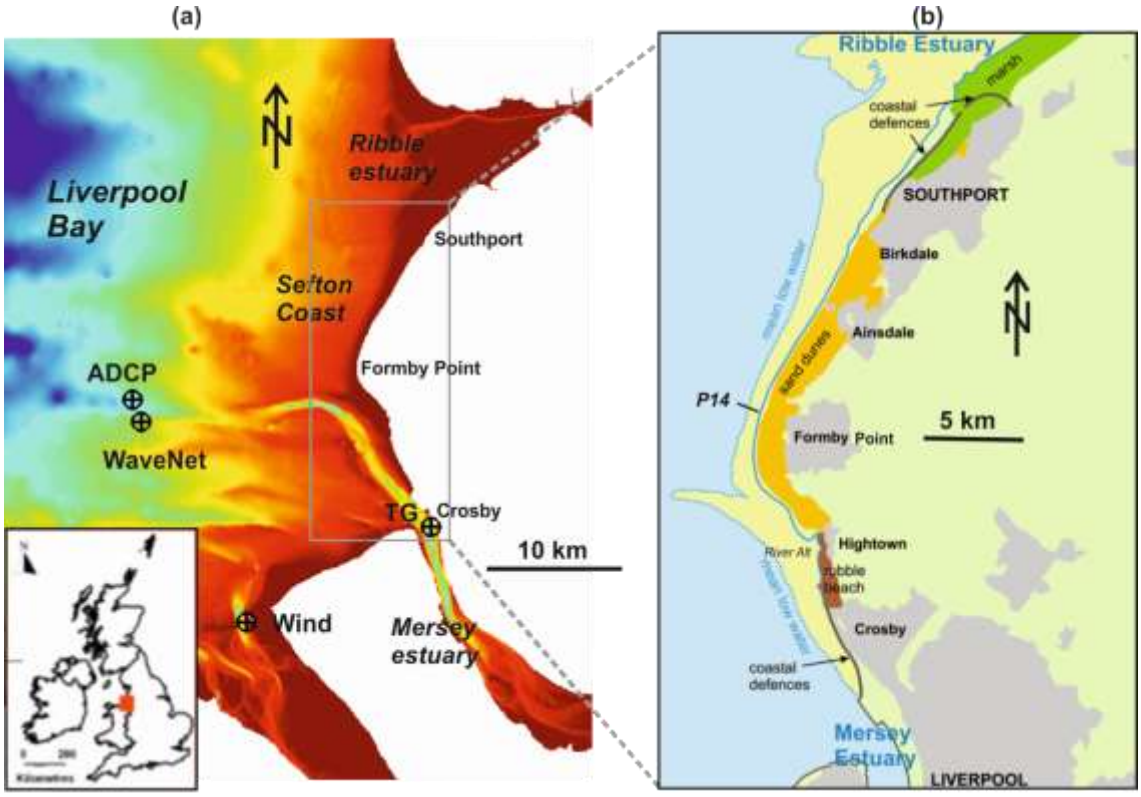

Figure 1 (a) Location of Liverpool Bay and Sefton coast with data observation points; ADCP (offshore tide), WaveNet (offshore wave characteristics), TG (Liverpool Gladstone Dock, nearshore tide) and Wind (Hilbre wind station) (b) a close-up of the Sefton beach system and the *P14* profile location.

The tidal regime at Liverpool Bay consists of an alongshore propagating semi-diurnal hyper-tide with a mean spring tidal range reaching about 8.2 m at Liverpool Gladstone Dock (see location *TG* in Figure 1a) (Brown et al., 2010a; Palmer, 2010; Blott et al.,

2006). Using long term wave measurements at an offshore location in Liverpool Bay (see location *WaveNet* in Figure 1a), Brown et al (2010b) simulated an 11-year wave hindcast which suggests a mean annual significant wave height (H_{m0}) of 0.5 m, with extremes reaching 5.6 m. The mean annual peak wave period (T_p) is 5 s while extremes are about 22 s. Positive surge in the area is often less than 0.5 m, however, during stormy conditions extreme surges of 2.4 m have been recorded along the Sefton coast (Brown et al., 2010a). The largest surges generally occur during lower water levels (i.e. rising tide). The maximum surge recorded at high water (i.e. 5.6 m) in Liverpool Bay is about 2 m in 1976 (Brown et al., 2010a). The largest wave conditions are associated with west to north-west winds where the longest fetch exists (Wolf et al., 2011).

Sediment characteristics of the Sefton coast are determined by inflow of the Mersey and Ribble estuaries, in addition to the net onshore drift due to the tides (Pye and Blott, 2008). Sediment composition in the nearshore area varies from about 0.1 mm to 0.3 mm in median grain size (D_{50}) (per. comm. with Sefton Metropolitan Borough Council). However, sediment information in the beach/dune system is very scarce. An average sediment size of 0.2 mm is used for the entire domain in the present model runs. The inter-tidal area of the Sefton coast has a ridge runnel system, which extends about 3 km seaward over a beach profile with a very mild slope of about 1:100 (Plater and Grenville, 2010).

The primary mechanisms leading to dune erosion are the soaking of the dune toe and then wave undercutting which can lead to slumping of the dune face and dune retreat (Pye and

Blott, 2008; Parker, 1969). The Sefton dune foot is located just above the mean spring high water level. Therefore, dune erosion occurs when extreme storm surge and wave events coincide with the spring-high tide. However, there is a potential for significant erosion during storm surges with high wave energy (Halcrow, 2009; Pye and Blott, 2008). Smaller storms erode only part of the Sefton coast while erosion of the entire dune frontage is possible during the most severe (> 1 in 10 year) events (Pye and Blott, 2008).

Metocean conditions in Liverpool Bay together with the shape of the coastline (i.e. convex shape) and the beach slope result in different morphological evolution along the Sefton coast. Some parts experience erosion while others accrete with different rates and trends (Esteves et al., 2012; Pye and Blott, 2008; Pye and Neal, 1994). The area around Formby Point (see Figure 1b) is highly dynamic. Prior to 1900, this area suffered seaward progradation, however it turned into an eroding system around the beginning of the 20th century (Pye and Neal, 1994; Pye and Smith, 1988; Gresswell, 1953). Local beach/dune erosion at Formby Point delivers sediment to the accreting shorelines both northward and southward (Halcrow, 2009; Pye and Blott, 2008; Pye and Neal, 1994). As a result, Formby Point presently acts as a divergent sediment cell boundary. Esteves et al (2009) found that the annual dune retreat north of Formby Point is about 5 m during the period from 2001 to 2008 and the erosion extends up to the River Alt area (see Figure 1b).

3. Storm event

A storm event that occurred between 29 March 2009 and 01 April is modelled in this study. The selection of this event was purely based on the availability of pre-storm (Sefton Metropolitan Borough Council) and post-storm (Williams et al., 2011) beach profile measurements for model calibration. It should be noted that even though a significant number of profile measurements are available for the Sefton coast, the timing and frequency of surveys prevents accurate pre and post storm observations, limiting their use for the current modelling purpose. In order to find out the severity of this storm event a comparison of its estimated storm power (Dolan and Davies, 1994; Karunarathna et al., 2014) with all historical events between 2003 and 2011was made. This analysis categorised the presented event as '*medium*' severity.

The measured meteorological conditions (tide, wave and wind) in Liverpool Bay are shown in Figure 2 for the period from 27th March to 05th April 2010. Tidal elevations are shown for two locations, an offshore point at 24 m ODN depth (i.e. see location ADCP in Figure 1a) and a tide gauge station inside the Mersey estuary (i.e. Liverpool Gladstone Dock tide gauge, see location TG in Figure 1a). The tide gauge data represents nearshore water levels for the Sefton coast while the ADCP provides offshore water level variations, which are later used as model boundary forcing (see section 5.1). Both water level time series are referenced to mean sea level (MSL) (see Figure 2a). Observations indicate that Liverpool Bay experiences spring-tides during this period. Differences in amplitudes and phases of these two tidal signals are expected due to the effects of local bathymetry in the shallow area and the geometry of the Mersey estuary (Dronkers, 2005).

Wave characteristics during this period are determined from the Liverpool Bay WaveNet buoy (i.e. Directional Waverider MkIII, serial number 30897) located at 24 m ODN depth (see location WaveNet in Figure 1). Significant wave height (Hs) shows a double-peak of which the maximum occurs on the 31st March (Figure 2b). The maximum recorded Hs of this storm is 3.80 m as it approaches from a north-westerly (NW) direction (i.e. 318^{0}, see Figure 1b). Occurrence of this wave height is marked with a dash-line for all parameters in Figure 2. According to the tidal elevations, the maximum wave height coincides with High Water (HW) (i.e. 4.76 m ODN at Gladstone Dock). The position of the dune toe generally lies slightly above the mean high water spring level (MHWS ~ 4.39 m ODN) and slightly increases towards the Ribble Estuary (Pye and Blott, 2008). Therefore, it can be expected that the dune toe may be subjected to soaking depending on the local morphology and the total water level while exposed to wave attack. At lower tidal phases strong local winds (i.e. wind speed is about 20 m/s, see Figure 2c and gusts exceeding 25 m/s, not shown), blowing from a NW direction (320^{0}), develop more aggressive wave action on the beach/dune front. Such a combination of forcing conditions (i.e. tide, wave and wind) is expected to result in significant morphological changes along the Sefton coast. It is noted that the occurrence of high waves coincidental with HW and a strong winds is not typically found in the historical in Liverpool Bay storm records (Esteves et al., 2012). Therefore, the present storm event is considered appropriate to undertake a morphological investigation.

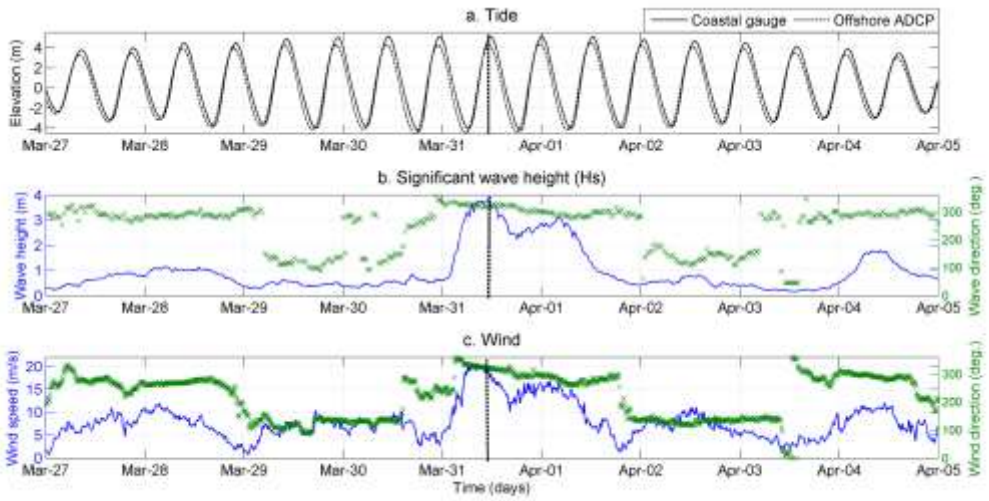

Figure 2 Variation of meteorological conditions from 27 March to 05 April 2010; Tide (a), Significant wave height (b) and wind (c). The vertical dashed-line represents the peak of the storm event.

4. Model setup

A nested modelling approach is setup in order to optimize the computational time and accurately represent the nearshore topography (i.e. beach/dune system). Our study primarily applies the XBeach model (Roelvink et al., 2009) to investigate the storm impact on the beach/dune evolution while the SWAN (Booij et al, 1999) and Delft3D (Lesser et al., 2004) models are implemented to establish boundary forcings. The Delft3D model is used to develop spatial and temporal varying sea surface elevations and velocity fields. These parameters are subsequently applied into the SWAN model in order to

transform offshore waves up to the XBeach model boundary imposing wave-current interactions under real-time water levels.

4.1 Model domains

One – dimensional (1D) model domain

The sensitivity tests described in section 4.4 use a 1D approach to simplify the situation and to minimise excessive computation times to evaluate the large number of model parameters involved. Even though this approach has some consequences, the cross-shore profile used for the sensitivity analysis is considered as a representative profile of the Sefton beach (see Figure 1b, *P14* is located at Formby Point) due to two main reasons. Firstly, it is located at a point of diverging alongshore sediment transport, so is representative of the cross-shore sediment dynamics, and is in a highly dynamic area of the Sefton coast, which undergoes strong morphological change compared with other locations along the coast (Esteves et al., 2012; Pye and Blott, 2008). Secondly, only this profile has measurements that extend up to about -8 m ODN depth. All other profiles have the seaward measurement limit up to about -2 m ODN only.

A pre-storm cross-shore profile at *P14* measured on the 14th March 2010 was established using available historical profile data from 1996 to 2010 and LiDAR data (Gold, 2010). The profile data are measured by the Sefton Metropolitan Borough Council, with the

addition of the event-scale monitoring undertaken by the MICORE project (Williams et al., 2011) for this case. These latter profile measurements have a cross-shore resolution of minimum of 5 m in the beach/dune area. The nearshore beach/dune profile (from dunes to -2 m ODN depth) was defined by the pre-storm LiDAR data which has a resolution of 1 m × 1 m in horizontal and about ±15 cm uncertainty in vertical. The profile from -2 m to -8 m ODN depth was determined from this historical data. The profile was then extended to -20 m ODN using a straight line (Figure 3). The profile consists of nearshore bar-trough patterns up to about -6 m ODN and a constant slope of about 1:500 thereafter. The computation domain was extended up to an offshore depth of -20 m ODN in order to generate offshore boundary conditions accurately (per. comm. with Deltares XBeach team). The offshore grid resolution was selected as 10 m, while a higher grid resolution (~ 2 m) is used over the beach/dune area.

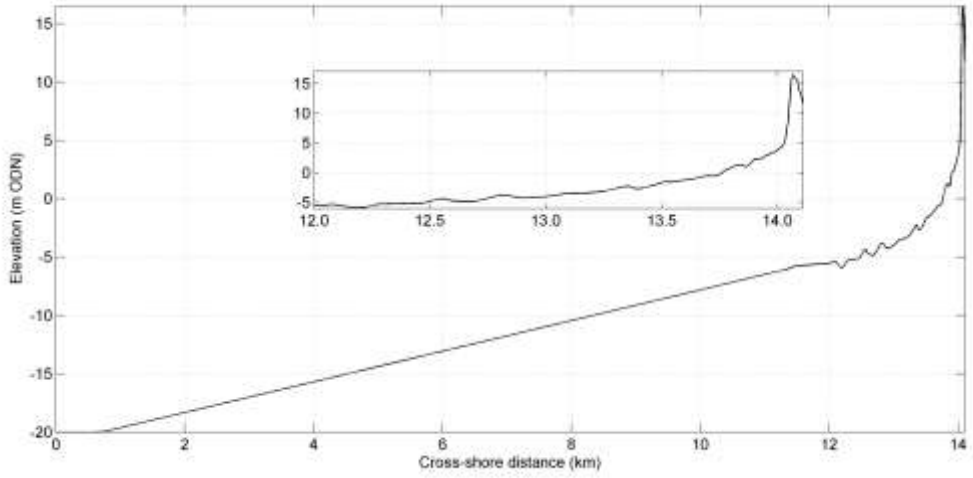

Figure 3 Established pre-storm 1D profile at location *P14* (see Figure 1) for the sensitivity analysis

382

383 *Two – dimensional (2D) model domain*

384

385 A 2D model domain is used for morphodynamic simulations of storm-induced beach
386 dune evolution. A nested modelling approach adopted in this study uses the *Sefton* and
387 *Formby* model domains as shown in Figure 4. The *Sefton* model domain is used to
388 transform offshore hydrodynamics (tides and waves) up to nearshore. Morphological
389 changes around the Formby Point area are investigated using the *Formby* model domain.
390 Both domains consist of curvilinear grids which follow the convex shape of the Sefton
391 coastline and the dune topography. Grid resolution in both models was varied across the
392 domain in order to achieve higher resolution in the areas of interest. The spread of the
393 offshore boundary is designed to capture all incident wave directions influencing this
394 coastal stretch.

395

396 The *Sefton* domain is established in both Delft3D and SWAN in order to provide water
397 level, velocity and wave boundary conditions for the smaller *Formby* domain. The latter
398 extends from Crosby (in the south) to Southport (in the north) covering a stretch of about
399 26 km representing almost the entire Sefton coast (Sefton grid in Figure 4). The location
400 of the offshore boundary is based on the Liverpool Bay *WaveNet* buoy (see Figure 1) of
401 which measured wave data are imposed in the SWAN model. Accordingly, the lateral
402 extension of this model is about 23 km offshore and the length of the offshore boundary
403 is about 45 km. Fairly coarse grids are applied in both *x* and *y* directions (minimum grid
404 25 m × 650 m and maximum grid 300 m × 800 m) compared with the *Formby* model as

405 this is only applied to transform offshore hydrodynamic characteristics (i.e. waves and
406 tides) for the XBeach simulations.
407
408 The *Formby* model domain covers the highly dynamic beach/dune system around
409 Formby Point which extends about 12 km in the alongshore direction. The depth of the
410 offshore model boundary was defined by applying the depth of closure approach of
411 Hallermeier (1983), assuming that no morphological changes occur beyond this point (i.e.
412 $d_{doc,outer}$ < 15 m). This results in lateral extension of the model domain 15 km offshore.
413 High resolution grid cells (~ 2 m × 25 m in cross-shore × alongshore directions) are
414 applied in the beach/dune area in order to resolve the dune shape adequately into the
415 model while coarser grid cells (~ 150 m × 110 m) are used offshore. Such grid
416 arrangements optimize the computational time which is an advantage for morphological
417 simulations.
418

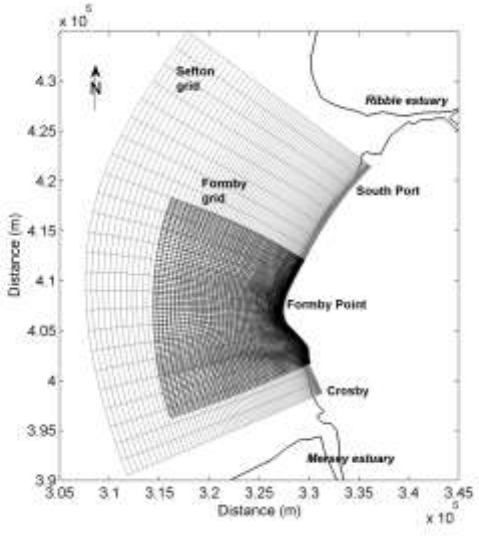

419

420 **Figure 4 Model domains applied in this study with the land boundary; XBeach finer grid setup**
421 **(Formby grid, dark grey) and Delft3D/SWAN coarser grid setup (Sefton grid, light grey)**

4.2 Sea bed bathymetry

Sea bed bathymetry and the dune topography for the 2D model were determined from the existing hydrodynamic model POLCOMS (Brown et al., 2010a) and the LiDAR data set (Gold, 2010) respectively. The 90 m resolution POLOCOMS bathymetry has been established using previous bathymetric data available in Liverpool Bay (i.e. from 2000 to 2008) and extends from the Sefton dune system (5 m ODN) to an offshore depth of about -50 m ODN (Williams et al., 2011). The LiDAR data set is based on the airborne laser scan transects observed on the 14th March 2010 (Gold, 2010). It has 1 m × 1 m resolution and covers the entire dune system up to about -2 m ODN depth. LiDAR data were re-gridded to 2 m × 2 m resolution to be used in our model. High resolution LiDAR data provides the model bathymetry from dune crest to -2 m ODN. The rest of the bathymetry (depth < -2 m ODN) was determined from the POLCOMS model bathymetry. The offshore boundary of the *Sefton* model is located at -25 m ODN (i.e. location of the *WaveNet* buoy, see Figure 1) while that of *Formby* was set at -15 m ODN (i.e. $d_{doc,outer}$ < 15 m) (Figure 5). It is noted that the offshore uniformity for boundary forcings is maintained in both cases by using a constant depth along the boundaries.

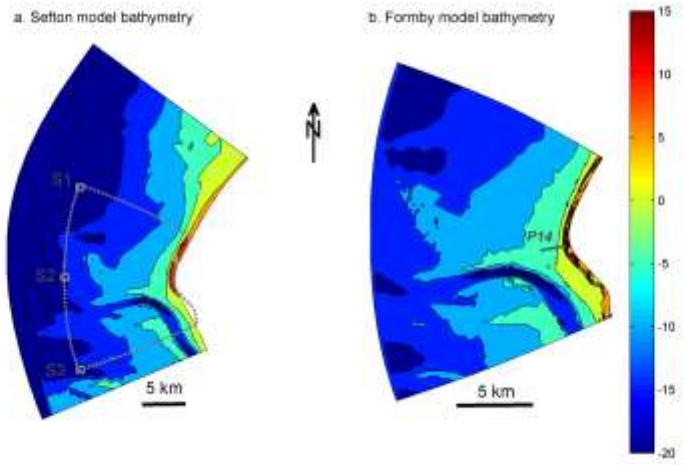

Figure 5 Model bathymetries developed based on LiDAR data and POLCOMS model bed for the *Sefton* domain (a) with outline of the *Formby* model and observation locations (S1, S2 and S3) , and *Formby* domain (b) with the location of profile P14

4.3 Boundary forcings

Boundary forcings for the model simulations were formulated in order to generate the hydrodynamic characteristics of the selected storm event (see Figure 2). The implemented real-time forcing conditions in this study are 1) *Tide*, 2) *Surge*, 3) *Wave* and 4) *Wind*.

Tide

459 The total water elevation boundary conditions for the *Formby* model were extracted from
460 those simulated by the *Sefton* model. The tidal boundary conditions for the *Sefton* model
461 were obtained from the ADCP data (see location *ADCP* in Figure 1a). It should be noted
462 that the alongshore propagating tide at Liverpool Bay has alongshore tidal phase
463 difference between the lateral (north and south) model boundaries. As there are no
464 observed data at the two lateral boundaries, the phase difference was estimated using
465 available POLCOMS model results in February 2008 (Bricheno et al., *in press*). Initially,
466 tidal elevations at the north and south points of the *Sefton* model were extracted from
467 POLCOMS . Each tidal signal was decomposed into tidal constituents applying a Fast
468 Fourier Transformation (FFT, i.e. observed sea surface is denoted by a number of tidal
469 constituents (~ 35) in their amplitude and phase differences) and then the corresponding
470 signals were reproduced for the same period using these estimated constituents (i.e.
471 Astronomical tide). Extracted tidal elevations from the POLCOMS results at north and
472 south points are shown in Figure 6 in comparison to the corresponding predicted
473 Astronomical tides which indicate sufficient agreement with the POLCOMS tide though
474 they imply marginally lower tidal range initially.
475

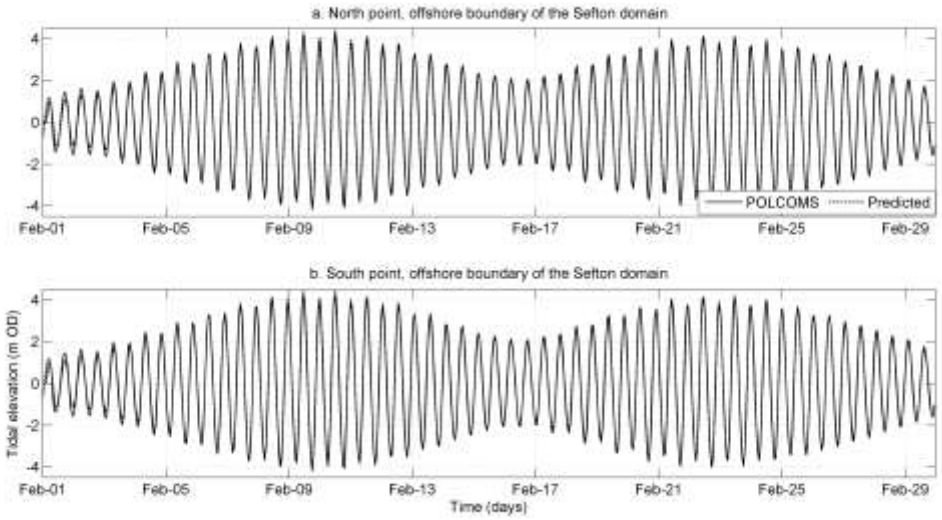

476

477 **Figure 6 Comparison of tidal elevations in February 2008 from POLCOMS results and Predicted**
478 **tide at north (a) and south (b) offshore points of the *Sefton* model**

479

480 These estimated tidal constituents (~35) are subsequently adopted to predict the tidal
481 elevations at those offshore points (i.e. north and south) during our study period (i.e. 27
482 March to 05 April 2010). These two signals indicated, tidal elevation at the north point
483 has a forward phase shift of 08 minutes and 38 seconds compared with that of the south
484 point, confirming an alongshore propagating tide (i.e. from south to north) at the coast in
485 this study area (Brown et al., 2010a). The ADCP provides observed total water depth at
486 the offshore boundary (i.e. 24 m ODN depth at ADCP, see Figure 1a) during the selected
487 storm event. For the storm event, these data were transformed into sea surface
488 fluctuations with respect to MSL by removing the long-term (10-year) mean (see Figure
489 7a). This approach allows the externally generated surge and tide to be included within
490 the boundary elevations along with interaction. Total water elevations at the north and
491 south offshore points of the *Sefton* domain were then determined applying the estimated
492 tidal phase shift to the observed water elevation (see Figure 7b). The ADCP data

represents tide, surge and any interactions that have occurred along fetches to this point. To capture any surge generation beyond this point the data is combined with tide gauge observations.. To do this the difference (-0.2 m) between the long-term mean water elevation and that during the storm event is used to bias the total time-varying water elevation during the storm period to remove the mean increase in water level due to the surge. By reconstructing a total time-varying surge component from tide gauge data, as described below, not only allows the locally generated surge to be included but also allows the total water elevation to be reference to ODN as required by the model. The resulting water elevations so far therefore include the spatially varying tide and the tide-external surge interactions relative to MWL.

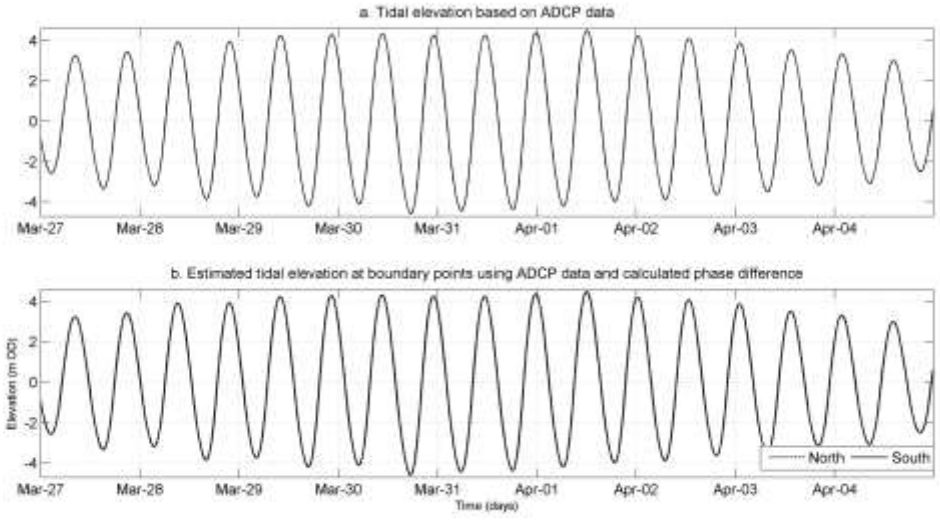

Figure 7 Measured ADCP data in the study period referring to MSL (a) and constructed tidal levels for north and south offshore points of the *Sefton* model (b). Note, a phase-shift of 08 minutes and 38 seconds between North and South boundaries is hard to differentiate.

Time-varying surge component

The surge boundary forcing was estimated based on the observed tidal elevations at the Liverpool Gladstone Dock tide gauge (TG in Figure 1a). The tidal elevation is referenced to CD so can be analysed to create a surge elevation relative to ODN. Initially, the observed tide was decomposed into 35 tidal constituents (i.e. applying FFT, see section *Tide* above). Then, the Astronomical tide was predicted for the same period. The observed elevation is the result of interactions between the propagating tidal wave, meteorological forcings and bathymetry, while the extracted Astronomical tide represents the sea surface variation without any local interference. It can be seen in Figure 8a that the observed total elevation is marginally higher and travels faster (i.e. forward phase shift) than the predicted tide. The difference between the two tidal signals is defined as the residual elevation (Figure 8b) at the gauge location. In the present analysis, the residual tide varies from -0.67 m to 1.29 m during the storm event and represents the total time-varying surge influencing the coast (Figure 8b). The 99^{th} percentile value of the long-term residual elevation (horizontal dash line in Figure 8b) indicates the threshold for extreme surge elevations which allow strong wave action on the dune front. The estimated (0.93 m) 99^{th} percentile value is exceeded twice (see grey vertical lines in Figure 8a and b) during the storm period at times that coincidence with the rising tide. It is typically found in Liverpool Bay that the maximum residual occurs during the rising tide rather than at HW (i.e. when the observed tide travels faster than the predicted Astronomical tide, see Horsburgh and Wilson, 2007). It is incorrect to superimpose this

residual elevation on to the offshore estimated total elevations (see Figure 7b) to incorporate the surge into the model boundary forcings because any tide-surge interaction occurring prior to the ADCP location would be double counted. To obtain the total time-varying surge component without tide-surge interaction the observed water level at the tide gauge was screened with a low-pass filter (see Dissanayake, 2011) to remove all oscillatory components occurring within a tidal period (i.e. 745 minutes). The resulting filtered surge varies between -0.09 m to 0.31 m in this storm event (Figure 8c) and represent the time-varying MSL of the region and can therefore be combined with the previously calculated water elevations (from the ADCP data) to represent the full tide-surge conditions.

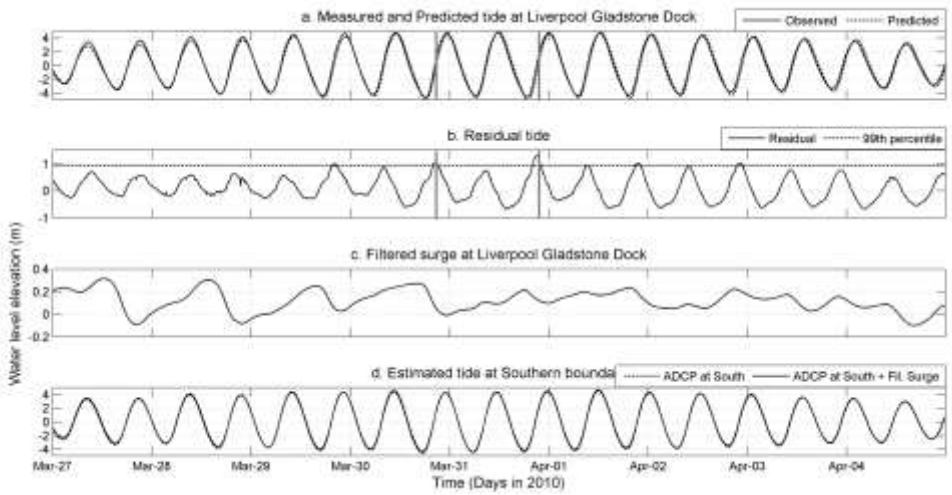

Figure 8 Estimating tide and surge elevation for the model boundary; Measured and Predicted (Astronomical) tide at Liverpool Gladstone Dock (a), Residual tide (b), Filtered tide at Liverpool Gladstone Dock (c) and Estimated tide and surge at southern boundary of Formby domain (d)

Waves

Offshore wave characteristics for the *Sefton* model boundary were derived using the measured wave data from the WaveNet buoy. Wave data are available from 2002 to present day (2013), covering an 11-year period. Analysis of this data set shows that the highest probability of occurrence is in the 270^0 to 300^0 directional sector (~WNW). Wave height rarely increases more than 5 m, typically exceeds 4 m during 1 – 5 events/year and 3 m during 5 – 10 events/year, while waves in the range of 0 – 1 m commonly occur each year. Wave characteristics during the study period (27 March to 04 April 2010) are shown in Figure 9a. The general trend of the long-term wave climate (i.e. from 2002 to 2013) is found even in this short period: High waves (> 1 m) occur in the North-West quadrant. The dominant wave direction (i.e. highest probability of occurrence) is from WNW whereas the highest waves (> 3.5 m) approach from a north-westerly direction.

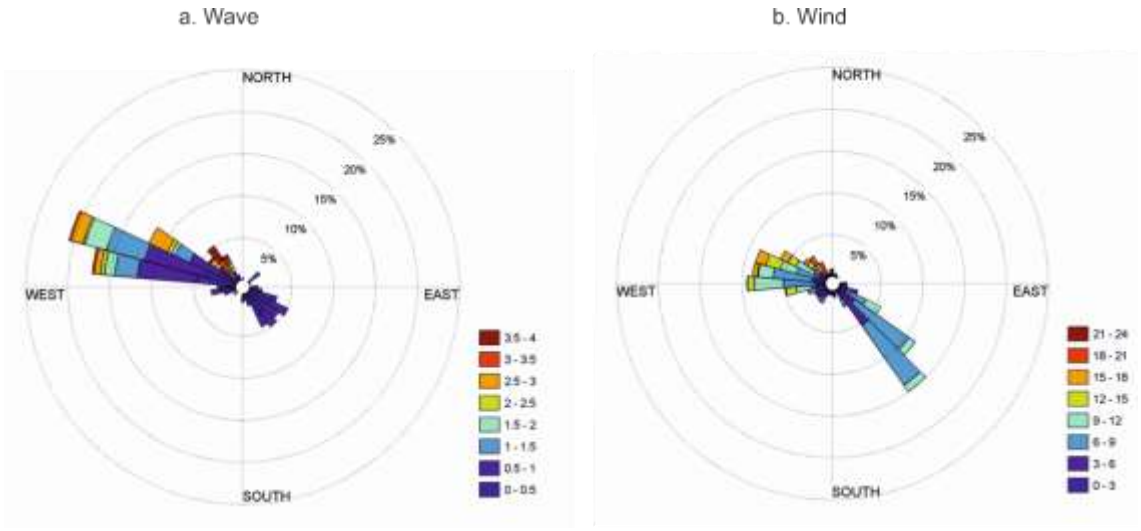

Figure 9 Wave and wind characteristics during the study period from 27 March to 04 April 2010; Wave rose (a) and Wind rose (b)

Wind

Wind forcing is applied to the *Sefton* (i.e. wave/tidal transformation) and *Formby* (i.e. morphological evolution) models based on observations from the Hilbre Island weather station (see location *Wind* in Figure 1) to generate local waves. Any wind driven surge generated within the model will be minimal due to small domains. The wind observation sensors are mounted at approximately 10 m above the ground on a tower which is above 16.5 m ODN. The wind rose in Figure 9b shows wind speed and direction during the study period. Strong winds (> 12 m/s) blow from the NW while wind speeds higher than 20 m/s approach from a NNW direction (~ 335^0). In contrast to the wave data, the dominant wind direction during the study period is from SE. This is due to the met station

being located at the mouth of the Dee estuary, which is aligned NW-SE, funnelling the local wind. Wind data are applied at each grid cell of both model domains (*Sefton* and *Formby*) such that they are spatially constant but temporally varying.

4.4 Model Simulations

Model simulations consist of three stages; 1) *Generating boundary forcings*, 2) *Sensitivity analysis* and 3) *2D area modelling*. The simulation length spans from 27 March to 04 April 2010. It is noted that the measured beach/dune topography at 14 March 2010 (i.e. re-gridded LiDAR data of 2 m × 2 m resolution) was considered as the initial pre-storm beach-dune topography. This is justified by the fact that incident wave conditions during 14th March and 27th March, where the storm occurred, are relatively mild (H_s < 0.5 m).

Generating boundary forcings

Hydrodynamic parameters (i.e. sea surface elevation and velocity fields) of the *Sefton* area are simulated for the study period applying the Delft3D-FLOW module. The SWAN model is used to simulate spectral wave parameters (i.e. H_s, T_p and *Direction*). Resulting sea surface elevation and wave conditions are extracted at the offshore boundary of the *Formby* domain to drive the high resolution *Formby* model setup in XBeach.

Sensitivity analysis

The XBeach model consists of a large number of model parameters. Morphological evolution is shown to be very sensitive to some of these parameters (McCall et al., 2010; Williams et al., 2011; Pender and Karunarathna, 2013). Therefore, a sensitivity analysis is carried out to tune a selection of model parameters, to be suitable for the Sefton coast. The 1D model domain described in Section 4.1 is used to carry out the sensitivity analysis (see Figure 3) and simulations were carried out for the storm period described above (i.e. 27 March to 04 April 2010). Each selected parameter is systematically changed with reference to the base case which represents the factory settings of the XBeach model (Table 1). Altogether, there are 18 simulations undertaken in the sensitivity analysis.

Model parameter	**Base simulation**	**Test No**				**Description**
		1	**2**	**3**	**4**	
wetslp	**0.3**	0.15	0.60	-	-	avalanching occurs when defined slope exceeded
smax	1	**0.8**	1.2	-	-	Maximum Shield value for overwash/sheet flow condition
form	1	**2**	-	-	-	Define transport formula, 1-Soulsby-Van Rijn and 2-Van Thiesel-Van Rijn
nuhv	**1**	10	20	-	-	Additional shear dispersion factor to create advective mixing
eps	**0.005**	0.001	0.025	-	-	Threshold depth for drying and flooding
morfac	**1**	2	3	4	5	Morphological scale factor
C	**57**	30	90	-	-	Chézy coefficient
facua	**0**	0.5	1.0			Calibration factor for wave asymmetry transport

Table 1 Model parameters and modified values in the 1D sensitivity simulations

2D area modelling

The high resolution *Formby* domain is used to investigate the storm induced morphological changes of the beach/dune system around Formby Point (i.e. the highly dynamic area on the Sefton coast). Model parameters in XBeach are tuned based on the sensitivity analysis described in section 4.4.2). The 2D simulation demands a large computational power due to the extent of the model domain (~ 12 km × 15 km), high grid resolution (min. ~2 m × 25 m) and the morphological simulation period (8 days). Therefore, the model runs are carried out on the Swansea University 'Blue Ice' HPC Linux Cluster, which has 600 CPU-core and 1.2TB RAM processing capacity.

5. Model results

5.1 Boundary forcings

Water level (WL)

The total water elevation predicted by the Delft3D-FLOW module at the offshore boundary of the *Formby* domain (*S1*, *S2* and *S3*, see Figure 5a) is shown in Figure 10. The mean water elevation at the offshore boundary of the *Sefton* domain (Bnd) and the observed tide (Tide) at the tide gauge (see *TG* in Figure 1) are also included in this figure for comparison. In the *Sefton* model domain (i.e. cross-shore extent ~ 20 km), the boundary water elevation is almost identical to that of the other locations; *S1*, *S2* and *S3*. However, the observed elevation is slightly different to the boundary forcing and the simulated elevation. The simulated elevation shows a better agreement during rising tide than falling tide, implying a forward phase shift (i.e. lag behind the boundary tide). The amplitude difference is higher at HW (max. ~ 0.8 m) than at LW. The tide gauge is located inside the Mersey estuary, which is outside of our model domain. Therefore, observed differences in phase and amplitude are expected due to the influence of local bathymetry and geometric change to the propagating tidal wave (Dronkers, 2005; Wolf, 1981).

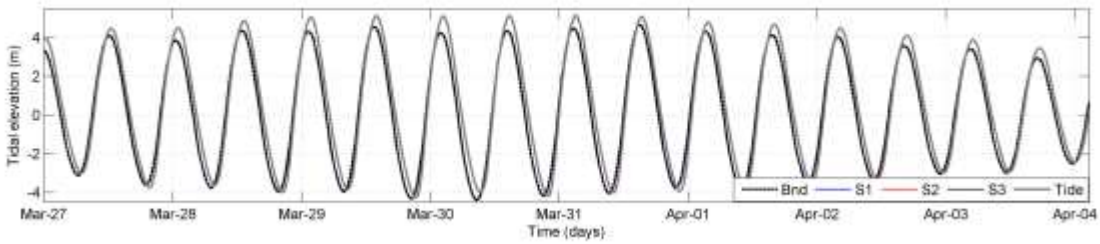

Figure 10 Comparison of predicted tide at S1, S2 and S3 of the *Sefton* domain with the boundary imposed tide (Bnd) and observed tide at the tide gauge (Tide) (see *TG* in Figure 1)

669

670 *Significant wave height (H_s)*

671

672 Evolution of the peak storm wave height (i.e. H_s = 3.8 m and dir. = 318^0 at 11:00 hours of
673 31st March 2010) for the SWAN simulation (see section 4.4), which occurs at HW (4.76
674 m ODN), is shown in Figure 11. The contours represent the total depth (MSL + HW
675 elevation) available for wave propagation at the peak of the storm. It can be seen that the
676 middle section of the Sefton coast (Formby Point and the surroundings) is exposed to
677 energetic wave conditions (~1.0 – 1.5 m). The northern and southern parts are subjected
678 to fairly low wave conditions due to a very shallow foreshore with multiple bar-trough
679 systems towards the north and shielding from the Crosby channel towards the south
680 leading to a high degree of wave dissipation. The dash-outline shows the extent of the
681 *Formby* domain. The offshore points *S1*, *S2* and *S3* marked in the *Formby* domain are
682 used to compare and contrast the predicted wave transformation with the waves at the
683 offshore boundary of the *Sefton* domain.

684

685

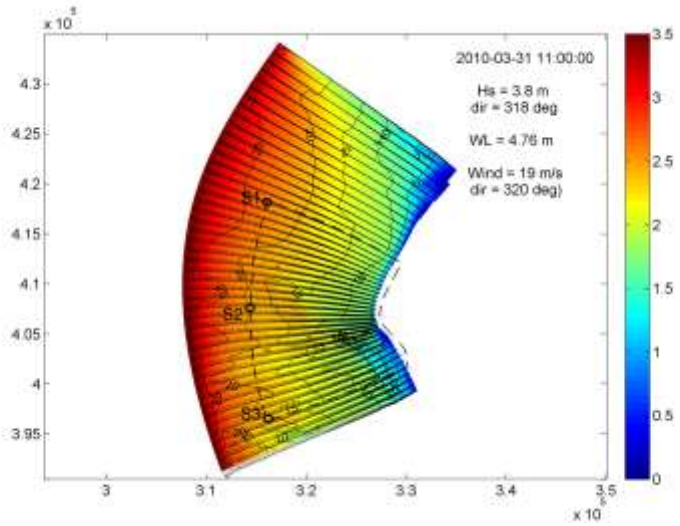

686

687 **Figure 11 Evolution of peak storm wave height across the *Sefton* model domain (Colour indicates**
688 **magnitude of H_s; Depth contours are drawn relative to the water surface; Dash-line shows outline of**
689 **the *Formby* model and offshore boundary points *S1*, *S2* and *S3*)**

690

691 Resulting waves (H_s, peak period (T_p) and direction) were extracted at offshore points
692 (*S1*, *S2* and *S3*) for comparison. The predicted H_s values at these locations are shown in
693 Figure 12 with the boundary wave (Bnd) applied at the offshore boundary of the *Sefton*
694 model (i.e. WaveNet data). Results indicate a general trend that higher waves (> 1 m)
695 dissipate and lower waves (< 1 m) grow while propagating from offshore to nearshore
696 areas. Along the offshore boundary of the *Formby* domain, the predicted wave heights
697 decrease from North to South (i.e. from *S1* to *S3*). This is mainly related to the sea bed
698 bathymetry of this area where water depth decreases from *S1* to *S3*. It should be noted
699 that the increment of H_s from *S1* to *S3* is marginal at low wave conditions. The largest
700 difference (~ 0.2 m) is found at the peak storm wave height.

701

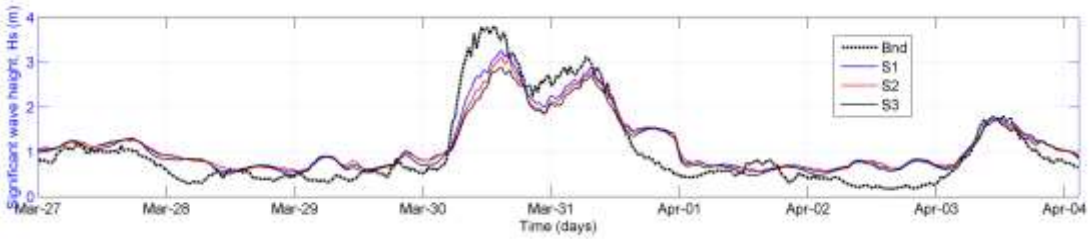

Figure 12 Boundary wave height of the *Sefton* model (Bnd) and transformed wave heights at the *Formby* model boundary; *S1*, *S2* and *S3* (see locations in Figure 11)

Predicted wave conditions at *S2* are subsequently employed to represent the offshore wave boundary conditions of the *Formby* domain.

5.2 Sensitivity analysis

Evolution of the 1D profile (see Figure 3) applying the modified model parameters is compared with that of the base case (see Table 1). Results are analysed in terms of Cumulative Volume Change, change in the beach/dune interface and Root Mean Square Error.

Cumulative Volume Change (*CVC)* for a unit alongshore length at each morphological time step was estimated by multiplying depth change and grid cell distance along the profile. Resulting *CVC* values of all sensitivity tests are shown in Figure 13 for the 8 day storm duration (i.e. 27 March – 04 April). In the first three days, results of the base case show no volume change due to very calm wave action (i.e. offshore H_s < 1 m, see Figure

12). After about 3.5 days, *CVC* increases up to about 3 m^3/m due to the first storm peak, and thereafter another increase (~1 m^3/m) occurs as a result of the second storm peak (see Figure 12). It can be seen that the morphological change of the base case is proportional to the magnitude of the storm peak wave height. This trend is found in all sensitivity test cases except in '*morfac*'. A summary of sensitivity analysis is given below:

wetslp: Avalanching occurs when the defined critical slope (*wetslp*) is exceeded. Higher slopes are expected to result in strong volume changes. In the present analysis, all applications (0.15, 0.30 and 0.60) show similar *CVC* values (Figure 13a).

smax: This represents the maximum Shield criterion for overwash and sheet flow conditions. Small values result in weak stirring and therefore less amount of sediment is expected to release into the water column leading to weak volume change. After the storm peak, *CVC* is proportional to the magnitude of *smax* (Figure 13b).

form: Sediment transport is estimated based on Soulsby-Van Rijn (1) or Van Thiesel-Van Rijn (2) formulations. After the storm peak, (1) estimates marginally low *CVC* compared with that of (2) (Figure 13c) due to inherent differences in both transport formulas (see Van Thiel de Vries et al., 2008 and Soulsby, 1997).

nuhv: This is an additional shear dispersion factor to create an additional advective mixing. Higher values increase the alongshore viscosity and then less amount of sediment

escapes into the water column. A marginal difference of *CVC* is observed after the storm peak (Figure 13d) which indicates the highest volume change applying the lowest value.

eps: Threshold depth for the drying and flooding algorithm is defined by *eps*. Small *eps* results in many wet grid cells, contributing to hydrodynamics and therefore increase in sediment transport compared to that of a large value. Sensitivity tests indicate similar *CVC* values under all three values (Figure 13e).

morfac: Application of the *morfac* value accelerates the bed level changes while decreasing the simulation period (Roelvink, 2006; Lesser et al., 2004). Systematic analysis of morfac selection is always recommended before applying a morfac value to investigate morphological changes (Dissanayake et al., 2009; 2012; Dissanayake and Wurpts, 2013). In the case of *morfac* tests, it was found that the bed evolution is mainly dominated by *morfac* value rather than the storm action. *morfac* = 1 shows relatively constant change (i.e. max. < 4 m^3/m). Application of 2 and 3 results in *CVC* more than 20 m^3/m while 4 and 5 show about 10 and -10 m^3/m volume change respectively at the end of the 8 day period. These results indicate that it is not realistic to apply higher *morfac* value (> 1) to accelerate the morphological evolution (i.e. to decrease the computational period) in the present analysis.

C: Smaller the Chézy coefficient the higher the bed roughness value imposing lower sediment transport rates. Our analysis shows, *C* = 30 has no positive change in *CVC* during the storm action due to very strong bed roughness compared to the cases of 57 and

90 (Figure 13g). The lowest bed roughness (C=90) results in the highest *CVC* (> 10 m^3/m).

facua: This parameter determines the contribution of wave asymmetry into the sediment transport. Sensitivity tests were undertaken applying no contribution (0), partial contribution (0.5) and fully contribution (1). However, they present almost similar *CVC* during the evolution (Figure 13h) implying that the wave asymmetry contribution on sediment transport is marginal in the situation considered in the present study.

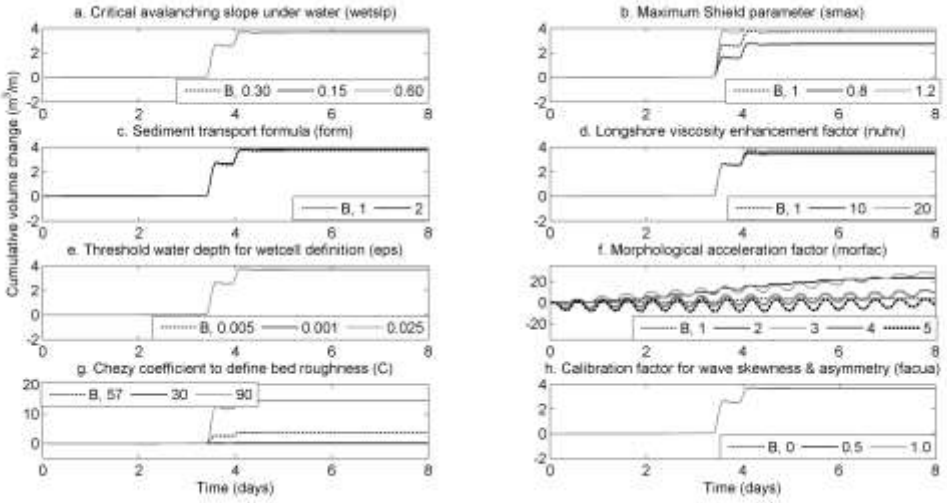

Figure 13 Cumulative Volume Change (*CVC*) (m^3/m) of the cross-shore profile (P14, see in Figure 3) in the Base case run and sensitivity runs (see Table 1 for Model parameters and modified values in the 1D sensitivity simulations)

Storm impacts on the beach/dune interface evolution are of special interest for the coastal managers in order to apply mitigation measures. In our sensitivity analysis, cross-shore variation of the beach/dune interface was estimated based on the 4.4 m ODN level. If water level reaches this threshold (note. tidal level exceeds 4.7 m ODN in the selected storm), a few meters of dune recession is expected under moderate waves within a single tide (Pye and Blott, 2008). Resulting dune recession values are shown in Figure 14 corresponding to the each sensitivity run. It is generally found that the model predicts about 4 m of dune recession, though some cases resulted in accretion at the beach/dune interface (see last two in '*facua*'). This provides a qualitative impression of the amount of the dune recession within the selected storm event.

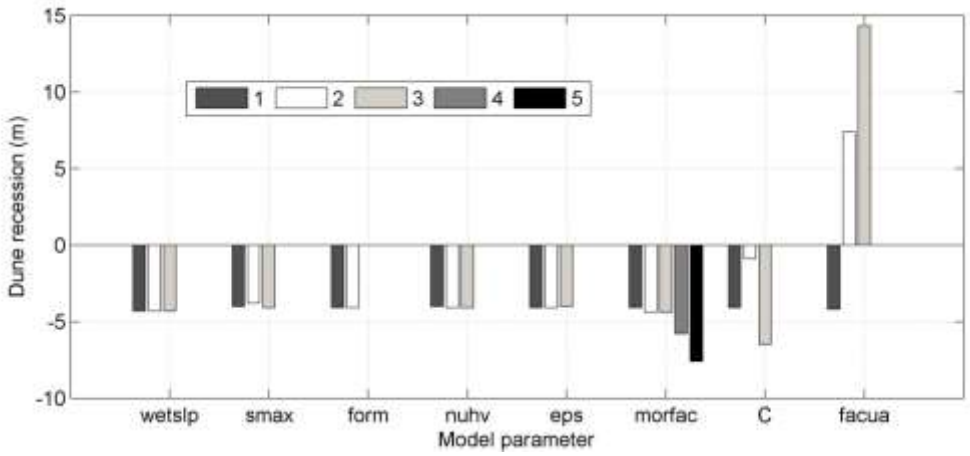

Figure 14 Change in the representative dune toe level (4.4 m ODN, Pye and Blott, 2008) in the cross-shore direction during the sensitivity runs with respect to the base case (see Table 1). Legend shows the test cases undertaken.

CVC and dune recession analyses provide relative impact of each coefficient and wave action on the beach/dune evolution along the storm duration. However, it is difficult to

802 determine the suitable coefficients for the study area based on the *CVC* alone, as the
803 measured profile length covers only a part of the simulated profile. Therefore, the Root
804 Mean Square Error (*RMSE*) between the simulated and measured profiles was also
805 calculated. In contrast to the *CVC* analysis, *RMSE* uses a portion of the simulated profile
806 (i.e. enclosing dune and beach areas) based on the measured profile length. *RMS*E is
807 given by *Eq 1* considering the changes at each grid cell of the selected profile length.
808
809

$$RMSE = \sqrt{\frac{\sum(z_{measured} - z_{predicted})^2}{N}} \quad (1)$$

810
811
812 where; $z_{measured}$, measured post-storm profile depth; $z_{predicted}$, predicted post-storm profile
813 depth and *N*, number of grid cells. The lower the *RMSE* the higher the agreement
814 between measured and predicted profiles.
815
816 Computed *RMSE* values are shown in Figure 15 for the base case and the different test
817 cases carried out. The sequence of bars is referred to the test number in Table 1. Each
818 cluster of bars represents the sensitivity of bed evolution to the modified values of the
819 respective coefficients.
820
821 The change of first five coefficients (*wetslp*, *smax*, *form*, *nuhv* and *eps*) induced a
822 marginal difference of the *RMSE*, which implies the fact that the sea bed evolution is not

significantly sensitive to these parameters. The last three clusters (*morfac*, *C* and *facua*) give relatively higher variability in *RMSE* indicating that the profile change is more sensitive to these model parameters than the others. The optimal value for each coefficient, which gives the lowest *RMSE* (see bold figures in each test case in Table 1) was selected for the 2D simulations given in Section 5.3. Accordingly, *smax* and *form* require adjusted values while all others remain as the default settings, which were implemented in the base case simulation.

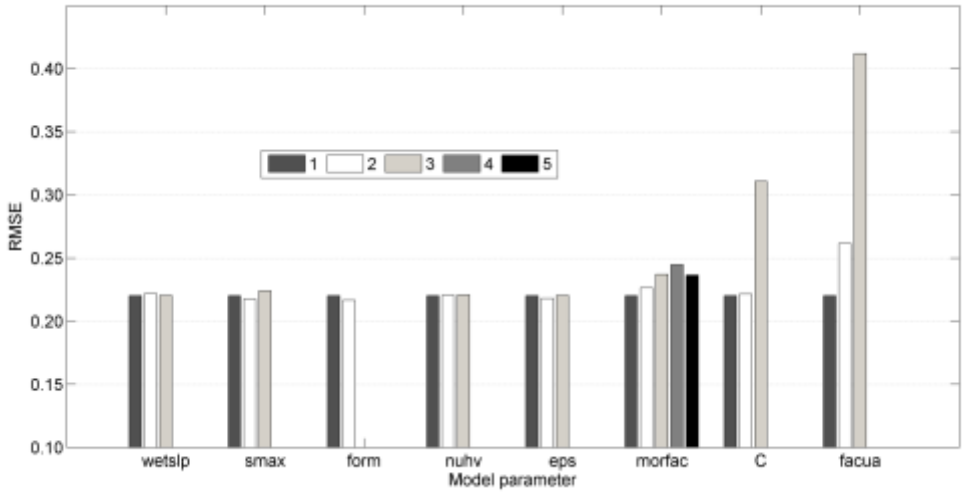

Figure 15 Estimated *RMSE* of sensitivity runs with respect to the Base case. Legend shows test cases undertaken in each parameter

5.3 Evolution of the beach/dune system

Application of the morfac value

A 2D morphodynamic simulation in the *Formby* domain requires about 1.6 days of a computational time on the HPC Linux cluster due to the finer grid resolution and the length of the morphological period (from 27 March to 04 April 2010). Therefore, potential application of the *morfac* value was further investigated. 2D morphodynamic simulations were carried out for the entire storm duration using *morfac* values of 1, 2, 3, 4 and 5). In addition, the *morfac* = 0 case (i.e. no morphological changes) was investigated to estimate the sediment influx into the model domain from the open boundaries.

Volume change of the model domain during the morphological period was estimated by multiplying bed level change of each grid cell by the area of the cell. Positive volume change implies sediment gain while negative change shows sediment loss from the system. In the simulations, all three open boundaries (i.e. north, south and west see in Figure 5) were set to have equilibrium sediment concentration (Galappatti, 1983) which allows sediment input/output based on the estimated concentration during the evolution. At each time step, the boundary sediment supply was computed by using the increment in grid cell size, to represent the distance along the boundary, multiplied by the corresponding sediment component perpendicular to the boundary. Then, the total sediment supply was calculated by as the sum over all time-steps. The estimated volume change and boundary sediment supply are shown in Figure 16 for all *morfac* applications.

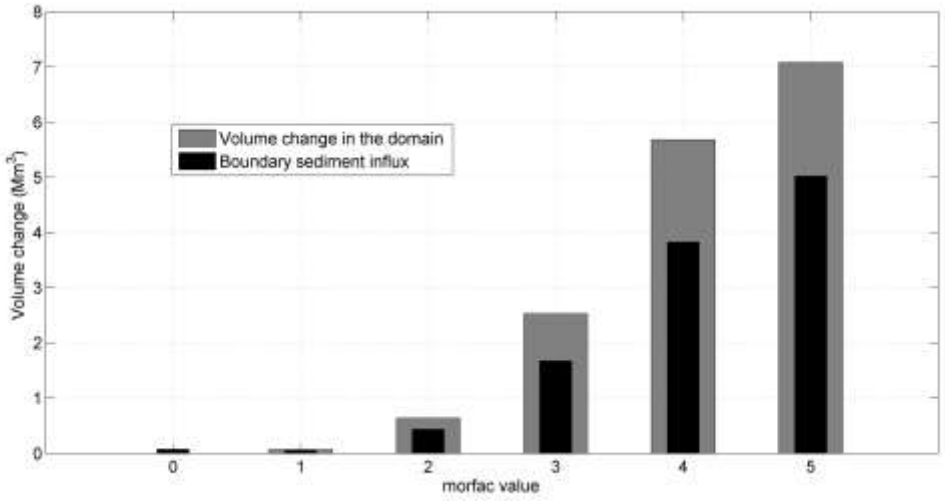

Figure 16 Comparison of mass-conservation with different *morfac* applications; Volume change in the model domain (grey) and Boundary sediment input into the domain (black)

They indicate sediment is being received into the system; a positive boundary input. It should be noted that the volume increase in the domain should be equal to the boundary sediment input in order to satisfy the mass conservation during the morphodynamic evolution.

The *morfac* = 0 case shows the boundary sediment influx into the model domain, indicating that the domain receives sediment from outside. For all non-zero *morfac* applications, volume change is not equal to the boundary sediment influx, which indicate mass conservation is not fulfilled. The lowest difference between volume change and boundary sediment influx (0.02 Mm^3) is found when *morfac*=1 is used and the highest (2 Mm^3) for *morfac*=5. It may be argued that the smallest difference (0.02 Mm^3) may occur as a result of errors arising from average depth considerations of a grid cell in the estimation of the volume change and therefore, considered as acceptable. The differences

879 between boundary sediment influx and volume change in the domain is significantly
880 large and is unacceptable for the *morfac* > 1 cases. Additionally, the erosion and
881 sedimentation patterns show unacceptably large changes along the dune front and at the
882 offshore boundary (not shown) as the *morfac* increases. Therefore, we use *morfac*=1 for
883 all simulations herein.
884
885
886 *Erosion and sedimentation pattern*
887
888 Morphological change in the *Formby* domain from the 27th March to 04th April 2010 is
889 shown in Figure 17. Initial depth contours at 5 m intervals are also shown in the same
890 figure for clarity. Significant bed level changes in the range of – 0.5 m (erosion) to 0.5 m
891 (deposition) are found mainly in two areas of the domain; 1) beach/dune system between
892 Southport and Formby Point and 2) north of the Crosby channel. These patterns provide a
893 qualitative indication of the interaction between storm driven hydrodynamic forces and
894 the bed morphology.
895
896 The strongest bed level changes seem to appear along the coastal stretch between
897 Southport and Formby Point. According to the direction of the peak storm wave height
898 (NW) and the orientation of the Sefton coast, it is evident that this area is more
899 susceptible to the wave action. The maximum recorded WL of this storm is about 4.8 m
900 ODN which could result in soaking of the dune foot and wave under cutting at the
901 proximity of +5 m contour (see erosion patches adjacent to this contour in Figure 17).

This is more pronounced at north compared with that at south of this stretch because the beach/dune system at north is exposed to stronger waves (see Figure 11during peak storm wave height). Bed evolution indicates alternate areas of erosion and sedimentation (i.e. forming runnels and ridges respectively) which are almost aligned with the initial depth contours. These are typical morphological features found after a storm attack on a sandy beach/dune system (Roelvink et al., 2009; Plater and Grenville, 2010). The significance of these features gradually decreases from the dune front towards the offshore, indicating strong morphological evolution of the dune front.

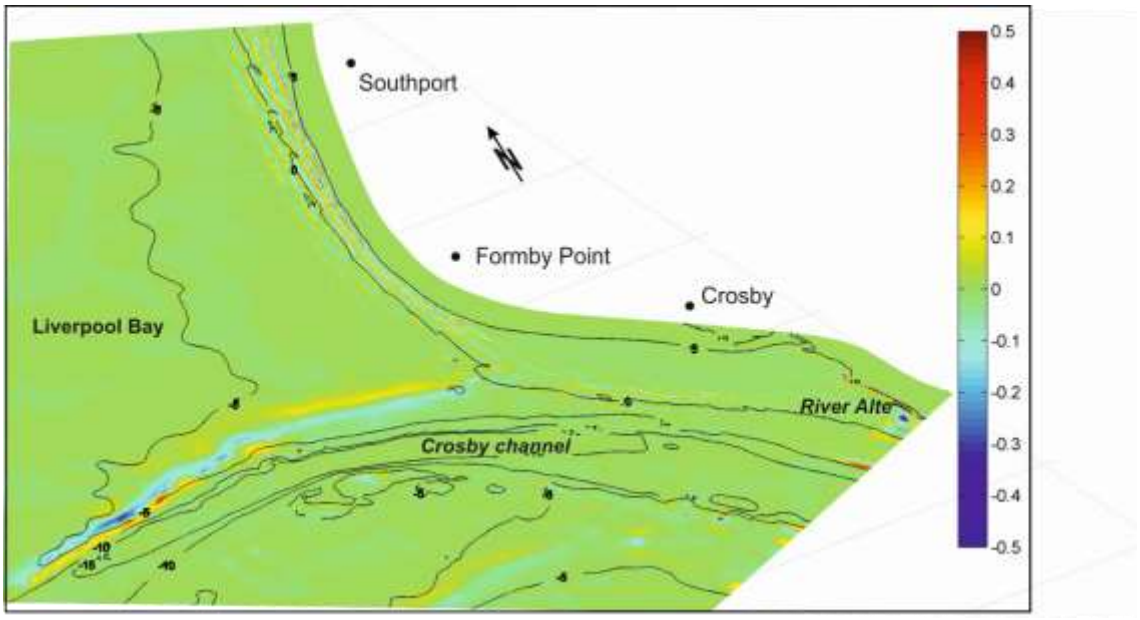

Figure 17 Erosion (blue) and Sedimentation (red) during the March 2010 storm event (from 27 March to 04 April). Contours indicate the initial bed topography

The seaward extension of the 5 m depth contour along the north bank of the Crosby channel implies a sand ridge on the initial bed topography. Such a shoal area interrupts

the NW incoming waves, which can lead to strong wave breaking in that area. This process may result in large bed level changes in the neighbouring areas. The eroding area is aligned with the ridge, which shows maximum wave interaction and dissipation occurring at highest bed levels. The highest erosion is found at the seaward end of the ridge and the eroded sediment has subsequently deposited at the leeward side. However, at the proximity of MWL, weak erosion is found at leeward side of the ridge and deposition is at the windward side. This may be due to the tidal currents enhanced by the presence of the Crosby channel (Thomas et al., 2001). Therefore, the predicted erosion/sedimentation patterns provide a qualitative impression on which areas are more prone to storm impacted bed level changes along the Sefton coast.

Bed level changes are further analysed in order to find areas of weak and strong depth variations. Density of erosion and deposition points with respect to the depth contours indicates the significance of bed level change in different regions of the domain (see Figure 18). The depth contours from 0 to 10 m represent the dune area while 0 to -15 m represent the sea area (see *x* axis). The *y* axis shows the bed changes (erosion – negative and deposition – positive). Two-vertical dashed-lines mark LW and HW limits (i.e. inter-tidal range).

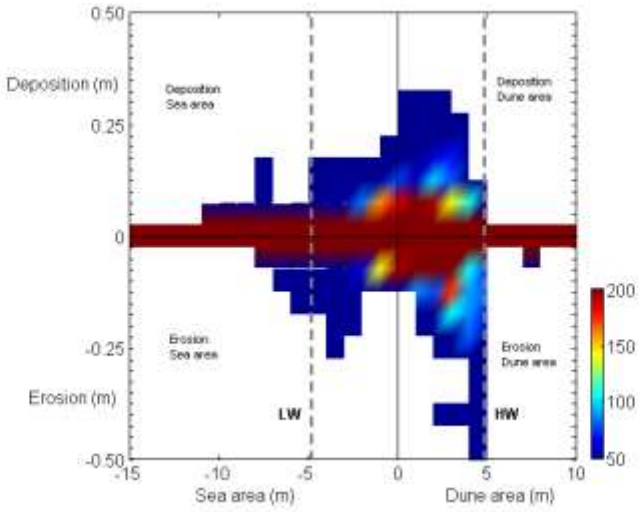

938

939 **Figure 18 Density of erosion and deposition points with the depth contours (see colour bar); LW and**
940 **HW indicate inter-tidal range in the domain; *x* axis shows depth contours while *y* axis indicates bed**
941 **level change.**

942

943 Four quadrants in Figure 18 show deposition/dune area, erosion/dune area, erosion/sea
944 area and deposition/sea area. The highest density of bed level changes (> 200) is found in
945 the range of -0.025 to 0.025 m from the dune area to sea area (see around $y = 0$). The
946 intertidal region shows the most bed evolution in the domain. The area above MWL has
947 greatest erosion (~ -0.5 m) and deposition (~ 0.3 m). The greatest erosion occurs at the
948 dune front (i.e. see around 5 m contour). Density variation indicates that the eroded
949 sediment has been transported towards MWL as found with the alternate erosion and
950 sedimentation areas in Figure 17. The strongest deposition is shown in between 0 and 3 m
951 contour levels. Below MWL, there are some areas which are subjected to relatively high
952 erosion and deposition and they may be related to the locations of sand ridges in the
953 initial sea bed.

954

955

956 *Profile evolution*

957 Post-storm profile measurements have been carried out on the 04th April 2010 (Williams
958 et al., 2011). These survey data cover the upper beach profile of the Sefton coast from
959 about 0.5 m ODN to the dune frontage. Five representative profile locations were used in
960 order to compare the measured and predicted storm induced bed evolution. These profiles
961 are shown on the beach/dune topography of the model domain (note. part of the Formby
962 model domain is present in Figure 19 for clarity). The 5 m depth contour demarcates
963 beach and dune area. The first three profiles (P12, P14 and P15) present the highly
964 dynamic area of the Formby Point which has the highest dune crests (max. height > 20 m
965 ODN). P12 and P14 run through these higher dune areas (> 15 m ODN) while P15 has a
966 relatively low dune height (< 15 m ODN). At P17, the profile indicates the lowest dune
967 crest height (< 10 m ODN). At the north of the dune system, there is a linear dune row
968 (max. height ~ 20 m ODN) parallel to the 5 m depth contour. The fifth profile, P18, is
969 located across this dune row.

970

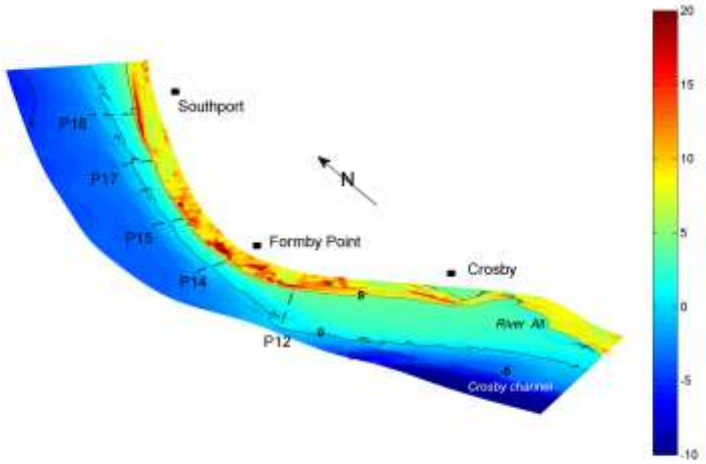

971

Figure 19 Selected profile locations (P12, P14, P15, P17 and P18) to compare measured and predicted bed evolution. Beach/dune system is shown with the depth contours (-5, 0 and 5 m ODN) and the topography (see colour bar).

Initially, the model predicted evolution at the selected profile locations was analysed with respect to the initial model bathymetry. As discussed in the 1D sensitivity runs, change in the beach/dune interface (i.e. dune recession) was estimated based on the 4.4 m ODN level (see Table 2). The highest dune recession is at P17 where there are lower dune heights, while the lowest recession is found at P12 with higher dune areas. These predictions agree with Edelman (1968) who concluded that the dune recession is inversely related to the dune height. This indicates that the lower dune areas are susceptible to storm impacts and need more focus in implementing management strategies. Extent of cross-shore bed level change was estimated using the distance between the beach/dune interface and the seaward depth at which marginal changes are expected beyond this point. At Formby Point, cross-shore sediment fluxes extend to longer seaward distances (see P14 and P15) implying strong bed evolution compared with other locations. These results indicate that analytically derived closure depth value (< 15 m, see section 4.1) is not applicable to the entire coast and the profile P15 is highly influenced (i.e. largest closure depth) by the alongshore sediment transport from Formby Point. These processes are further evident from the cross-shore volume changes along the Sefton coast (i.e. strongest negative volume change (erosion) is at the latter two profiles). It should be noted that using our 2D simulations, a similar analysis can be carried out for the entire Sefton coast. Results for a few selected cross shore locations are given in Table 2.

Profile No	Change in beach/dune interface (4.4 m ODN level) in cross-shore direction (m)	Extent of cross-shore changes		Cross-shore volume change (m^3/m)
		Closure distance from the 4.4 m ODN level (km)	Closure depth (m ODN)	
P12	-0.5	3.0	-8.6	-11.4
P14	-2.0	8.9	-10.1	-15.8
P15	-1.6	10.4	-10.3	-15.8
P17	-3.6	0.6	-3.0	-10.3
P18	-1.6	2.0	-5.6	-13.1

Table 2 Model predicted bed evolution at the selected profile locations with respect to cross-shore change of the beach/dune interface (4.4 m ODN level, Pye and Blott, 2008) (negative change is dune recession), cross-shore extent of bed level change and volume change for unit alongshore length (negative change is erosion).

Predicted morphological changes of these profiles were extracted from bed level changes in the 2D bed evolution simulations at the same locations of measured profile coordinates. The resulting profile evolutions during the storm period (i.e. initial and final predicted profiles) are shown in Figure 20 with the measured post-storm profiles. It is noted that the measured profiles cover only a part of the complete profile and only for the post-storm conditions. A comparison of measured and simulated profiles at these locations is given below:

a. Profile P12

Evolution of *P12* during March - April 2010 storm is shown in Figure 20a. This profile has a very gentle slope (>1:100) below the dune foot and indicates marginal changes

during the storm event. A good agreement between simulated and measured post-storm profiles can be seen, except at elevations higher than 5.5 m ODN. It should be noted that the measured profile segment spans from about 80 m to 230 m in seaward distance.

b. Profile 14

P14 has a very steep dune face (Figure 20b). Predicted results show a slight beach lowering at the dune foot and between 200 - 230 m cross shore distance. The measured profile spans from 100 m to 250 m. The predicted and measured post-storm profiles show an encouraging agreement.

c. Profile 15

Profile shape of the 2D model bed has ridge and runnel variations (see black-dash-line in Figure 20c). Predicted results show areas of erosion and accretion along the profile during the storms. Measured post storm profile segment spans about 100 m (from 175 m to 275 m) from 2.5 m ODN to 0.5 m ODN in elevation. The measured post-storm profile shows lower beach levels than the predicted levels.

d. Profile 17

The lowest dune crest height (< 10 m ODN) is found in *P17* (Figure 20d) compared with the other profiles. Measured post-storm profile segment has a length of about 160 m (from 90 m to 250 m). The predicted post-storm profile agrees well with the measured profile except between 130 m and 190 m chainages.

e. Profile 18

The highest dune elevation (17.2 m ODN) is found in *P18* (Figure 20e). The profile has three bars and troughs from 120 m to 600 m. Predicted results show erosion of the bars and deposition at the troughs. Measured post-storm profile extends from about 120 m to 260 m, covering a single bar and a trough. The predicted and measured post-storm profiles agree reasonably well except in an area around the crest of the profile.

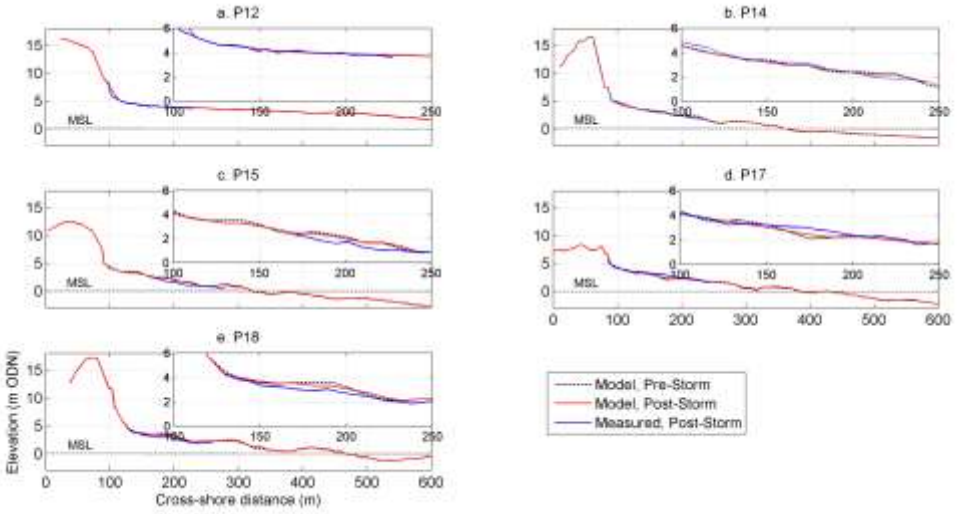

Figure 20 Comparison of measured and model predicted cross-shore profiles; P12, P14, P15, P17 and P18 (see locations in Figure 19); Model pre-storm (black-dash-line), Model post-storm (red-line) and Measured post-storm (blue-line)

To quantify the comparison of predicted and measured post-storm cross shore profiles, three statistical parameters, *RMSE*, Brier Skill Score (*BSS*) and Correlation coefficient (R^2) are used.

Averaged *RMSE* value was estimated as discussed in section 5.2. The lower the *RMSE*, the higher the agreement between predicted and measured profiles. Resulting *RMSE* values for each profile prediction are given in Table 3. The lowest *RMSE* (0.19) is found in the *P14* while the highest (0.39) is in the *P15*, implying that the *P14* and *P15* provide the best and the worst predictions respectively compared to the measured post-storm data. Both *P12* and *P17* result in RMSE of 0.34. The *P18* gives a *RMSE* of 0.29.

	Profile No				
Parameter	**12**	**14**	**15**	**17**	**18**
RMSE	0.34	0.19	0.39	0.34	0.29
BSS	0.88	0.96	0.84	0.87	0.90
R2	0.90	0.98	0.48	0.89	0.83

Table 3 Statistical comparison of measured and model predicted profiles (P12, P14, P15, P17 and P18) using *RMSE*, *BSS* and R^2

The *BSS* definition is given in *Eq*. 2 (Van Rijn et al., 2003). Van Rijn et al (2003) have classified the model predicted bed evolution according to the resulting *BSS* value (e.g. 0 – 0.3 *Poor*; 0.3 – 0.6 *Reasonable/Fair*; 0.6 – 0.8 *Good*; 0.8 – 1.0 *Excellent*).

$$BSS = 1 - \frac{\left\langle \left(z_{measured,post-storm} - z_{model,post-storm}\right)^2 \right\rangle}{\left\langle \left(z_{measured,pre-storm} - z_{model,post-storm}\right)^2 \right\rangle} \quad (2)$$

where, $z_{measured,\ post\text{-}storm}$, measured profile elevation after the storm; $z_{measured,\ pre\text{-}storm}$, measured profile elevation before the storm (i.e. initial model bed in the present analysis); $z_{model,\ post\text{-}storm}$, model predicted final profile elevations after the storm.

Resulting *BSS* values show the highest (0.96) in *P14* and the lowest (0.84) in *P15* while *P12* and *P17* have almost similar values (~0.88). *P18* has a *BSS* of 0.90. Therefore, the trend of *BSS* variation in each profile is similar to that of the *RMSE* values. According to Van Rijn et al (2003) classification, model simulations at all profiles qualify as '*Excellent'*.

The third statistical parameter used in this analysis is Correlation coefficient which is defined in *Eq*. 3. Higher R^2 values imply high degree of similarity between measured and model predicted profiles.

$$R^2 = 1 - \frac{\sum\left(z_{measured,post-storm} - z_{model,post-storm}\right)^2}{\sum\left(z_{measured,post-storm} - \left\langle z_{measured,post-storm} \right\rangle\right)^2} \quad (3)$$

The highest (0.98) and the lowest (0.48) R^2 values are found in *P14* and *P15* respectively R^2 values at *P12* and *P17* are almost identical (~0.90). R^2 value at *P18* is 0.83.

Even though statistical measures such as *RMSE, BSS* and R^2 gave very encouraging results for comparison of predicted profiles with the measured data, there are some discrepancies between the profiles. These can be attributed to two main reasons: slight mismatch of predicted and measured profile locations as measured profile information did not include coordinates; differences in profile resolution- predicted results are at a much higher resolution than the measured data.

6. Discussion

The LiDAR data (i.e. used to construct pre-storm bathymetry) and the observed post-storm profile data had different horizontal and vertical resolutions. This and some uncertainties regarding the accuracy of measurements may have caused some inaccuracies in the model predictions. This research, which is still continuing, is working alongside coastal managers, highlighting the observational needs for more detailed model validation; while understanding the model outputs required to advise regional monitoring schemes to maximise the usage of data collection for both management and research purposes. The aim is to ensuring science research is of benefit to coastal management addressing the gaps in knowledge.

To enable the longer term modelling, selection of the morfac value is required and is an entirely site specific process which depends on the local morphological and boundary forcing characteristics. Therefore, a sensitivity of bed evolution to morfac value should always be investigated prior to the selection of an optimum value for a given case study (Dissanayake et al., 2009; 2012; Dissanayake and Wurpts, 2013; Roelvink, 2006). Following this hypothesis, we systematically tested incremental morfac values (i.e. 1, 2, 3, 4 and 5) to find the most suitable value for the current application.

Present study is a part of an on-going 3-year research project in which the main focus is to investigate the impacts of storm clusters on the evolution of Sefton beach/dune system. The model setup used in this study will then be extended to investigate the beach profile response to storm sequences, in order to identify the contribution of storms on the long-term dune change.

The initial research presented suggests the northern part of the Sefton coast incurred stronger morphological changes than the southern part due to the direct exposure to NW peak storm waves of the selected storm. Resulting bed evolution of the beach/dune system indicated an alternate pattern of erosion and accretion areas, which is shown to be typical of the study area (Plater and Grenville, 2010). The shoal area located to the north of the Crosby Channel obstructs NW waves resulting relatively calm wave action on the southern part of the Sefton coast. As a result, morphological changes along the Crosby channel and on the adjacent dune system is significantly low.

Sediment exchange volumes between dune face and beach foreshore were quantified at selected cross-shore profile locations. This is useful to identify erosion prone areas along the Sefton coast. Further, the closure distance and depth were estimated based on the model predicted evolution which shows how far eroded material move seaward. It was evident that the beach/dune system of the Sefton coast has very complex spatial variability.

This study further provides important messages for the XBeach model user community. In addition to the dune system along the upper beach the lower beach of the Sefton coast consists of a complex ridge-runnel system, most likely due to the hyper tidal conditions. Present application shows the ability of the model to capture not only the morphodynamic variability of the upper beach but also the ridge-runnel system and the models ability to perform under such large tidal regimes. Most previously recorded XBeach applications were limited to straight line coastal systems. Here we demonstrated the ability of the model in capturing morphodynamics of a convex coastline, which confirms models ability to capture dynamics of diverse coastal system.

7. Conclusions

A numerical model study was carried out in order to hindcast the storm-induced dune evolution at the Sefton coast in the Liverpool Bay, UK, using a storm event that occurred

during March-April 2010. A nested modelling approach was used by combining a coarser model domain to transform offshore hydrodynamics (i.e. tides, surge and waves) up to the nearshore area and a fine-grid model to investigate the morphological evolution. Predicted bed evolution was analysed and compared with measured post-storm profiles available at a number of cross-shore locations along the beach in order to enhance the understanding of the potential storm impact on the Sefton beach/dune system. Results suggest following conclusions:

- Compared with many coastal locations, the Sefton coast has a rich set of information on tides, waves and morphological changes. However, if sediment transport data were also available, a better model calibration could have been done. Also, it should be noted that the storm event used in this study was not one of the extreme storms occurred in this region. However, we were restricted to use this storm at this instant due to limited availability of post-storm profile measurements for other larger storms.

- Wave model results indicate a general trend that higher waves (> 1 m) dissipate and lower waves (< 1 m) grow while propagating from offshore to nearshore areas.

- Morphological updating facility *morfac* available in the XBeach model (*morfac* > 1 approach) was not suitable to the prevailing environmental conditions of the Sefton coast (i.e. a hyper-tidal region).

- Resolution of the observed data (LiDAR data and post-storm profiles) and the uncertainties therein may have underestimated the model predicted bed evolution to some extent.

- H_s of the March 2010 storm shows a double-peak of which the maximum occurred on the 31st March due to higher wave and wind conditions approaching from WNW sector during rising tide, which resulted the greatest bed evolution on the Sefton beach/dune system.

- Comparison of pre- and post-storm dune-beach profiles at five cross-shore locations along the beach show that a small amount of dune face erosion occurred during the storm. However, it should be noted that the selected storm (max. H_s = 3.8 m) is not significantly severe compared with large storms that occur in this region (H_s ~ 4 m for 1 in 1 year event).

- Statistical comparisons (i.e. *RMSE*, *BSS*, R^2) suggested good agreement between predicted and measured post-storm profiles thus reassuring that the selected modelling approach is capable of satisfactorily predicting the morphodynamic evolution at the Sefton coast.

- Results on dune recession, cross-shore/alongshore variability of morphological changes and depth of closure values and distances of influence along the Sefton coast in the storm event scale provide useful qualitative information for coastal

managers, to update/revise conceptual maps of sediment fluxes that are used in current shoreline management practise.

- Results show the XBeach model's ability to simulate the complex ridge-runnel system of the lower beach in addition to the dune erosion along the upper beach in a hyper-tidal environment (i.e. spring-tidal range > 8 m).

- We demonstrated the potential application of the XBeach model for a complex coastal system (i.e. 2D convex coastline) though the model was initially developed for straight line coasts.

The present model study provides preliminary insights to the storm-induced morphodynamics of the Sefton coast dune system. These findings will have important implications on interpretation of the observed dune erosion at the Sefton coast and will be useful in formulating sustainable dune management strategies. On-going study extends this morphological model setup to estimate potential wave overtopping and flood risks during future single storm events and storm clusters.

Acknowledgements

The work presented in this paper was carried out under the project 'FloodMEMORY (Multi-Event Modelling Of Risk and recoverY)' funded by the Engineering and Physical Sciences Research Council (EPSRC) under the grant number: EP/K013513/1. Prof. John

Williams is greatly acknowledged for providing post-storm profile data, collected as part of the MICORE project (EU FP7 program Grant 202798). BODC, NTSLF and CEFAS (WaveNet) are acknowledged for providing tidal and wave data respectively. Sefton Metropolitan Borough Council is appreciated for the access of other relevant data used in this study.

References

Blott, S.J., Pye, K., Van der Wal, D., Neal, A., 2006. Long-term morphological change and its causes in the Mersey Estuary, NW England, Geomorphology 81, 185 – 206.

Booij, N., Ris, R.C., Holthuijsen, L.H., 1999. A third generation wave model for coastal regions, Part I, Model description and validation, Journal of Geophysical Research 104, C4, 7649 – 7666.

Bosboom, J., Aarninkhof, S.G.J., Reniers, A.J.H.M., Roelvink, J.A., Walstra, D.J.R., 2000. UNIBEST-TC 2.0 – overview of model formulations. Rep, H2305.42, Delft Hydraulics, Delft.

Bricheno, L.M., Wolf, J.M., Brown, J.M., *in press*. Impacts of high resolution model downscaling in coastal regions, Continental Shelf Research.

Brown, J.M., 2010. A case study of combined wave and water levels under storm conditions using WAM and SWAN in a shallow water application, Ocean Modelling 35, 215 – 229.

1259 Brown, J.M., Souza, A.J., Wolf, J., 2010a. An investigation of recent decadal-scale storm events in the
1260 eastern Irish Sea, Journal of Geophysical Research 115, C05018, doi: 10.1029/2009JC005662.
1261
1262 Brown, J.M., Souza, A.J., Wolf, J., 2010b. An 11-year validation of wave-surge modelling in the Irish Sea,
1263 using a nested POLCOMS-WAM modelling system, Ocean Modelling 33, 118 – 128.
1264
1265 Brown, J.M., Souza, A.J., Wolf, J., 2010c. Surge modelling in the eastern Irish Sea: Present and future
1266 storm impact, Ocean Dynamics 60, 227 – 236.
1267
1268 Brown, J.M., Wolf, J., Souza, A.J., 2012. Past to future extreme events in Liverpool Bay: model projections
1269 from 1960 – 2000, Climatic Change 111, 365 – 391.
1270
1271 Callaghan, D.P., Nielsen, P., Short, A., and Ranasinghe, R., 2008. Statistical simulation of wave climate
1272 and extreme beach erosion, Coastal Engineering 55, 375 – 390.
1273
1274 Carter, R., 1988. Coastal environments: an introduction to the physical, ecological and cultural systems of
1275 coastlines, Academic Press, London, UK.
1276
1277 Ciavola, P., Jimenez, J.A., 2011. The record of marine storminess along Europian coastlines, NHESS –
1278 Special Issue, http://www.nat-hazards-earth-syst-sci.net/special_issue135.html
1279
1280 Dissanayake, D.M.P.K., 2011. Modelling Morphological Response of Large Tidal Inlet Systems to
1281 Sea Level Rise, PhD Dissertation, UNESCO-IHE Institute for Water Education, Delft, the Netherlands.
1282
1283 Dissanayake, D.M.P.K., Ranasinghe, R., Roelvink, J.A., 2012. The morphological response of large tidal
1284 inlet/basin systems to Relative Sea Level Rise. Climatic Change, DOI: 10.1007/s10584-012-0402-z
1285

Dissanayake, D.M.P.K., Van der Wegen, M., Roelvink, J.A., 2009. Modelled channel pattern in a schematised tidal inlet, Coastal Engineering 56, 1069 – 1083.

Dissanayake, P., Wurpts, A., 2013. Modelling an anthropogenic effect of a tidal asin evolution applying tidal and wave boundary forcings: Ley Bay, East Frisian Wadden Sea, Coastal Engineering 82, 9 – 24.

Dolan, R., Davies, R.E., 1994. Coastal storm hazards, Journal of Coastal Research (Special Issue No. 12), 103–114.

Donnelly, C., Kraus, N., Larson, M., 2006. State of knowledge on measurement and modelling of coastal overwash. Journal of Coastal Research 965 – 991.

Dronkers, J., 2005. Dynamics of Coastal Systems, Advanced Series on Ocean Engineering – Volume 25, 235 – 240.

Edelman, T., 1968. Dune erosion during storm conditions, Proceeding of the 11th conference of Coastal Engineering, London, Volume 2, 719 – 722.

Edmondson, S.E., 2010. Dune Slacks on the Sefton Coast, Sefton's Dynamic Coast, Proceeding of the conference on coastal and geomorphology, biogeography and management, 178 – 187.

Erikson, L., Larson, M., Hanson, H., 2007. Laboratory investigation of beach scarp and dune recession due to notching and subsequent failure. Marine Geology 245 (1), 1 – 19.

Esteves, L.S., Williams, J.J., Nock, A., Lymbery, G., 2009. Quantifying shoreline changes along the Sefton Coast (UK) and the Implications for Research-Informed Coastal Management, Journal of Coastal Research, SI 56, 602 – 606.

Esteves, L.S., Brown, J.M., Williams, J.J., Lymbery, G., 2012. Quantifying thresholds for significant dune erosion along the Sefton Coast, Northwest, England, Geomorphology 143 – 144, 52 – 61.

Esteves, L.S., Williams, J.J., Brown.J.M., 2011. Looking for evidence of climate change impacts in the eastern Irish Sea, Natural Hazards Earth System Sciences, 11, 1641 – 1656.

Galapatti, R., 1983. A depth integrated model for suspended transport. Report 83-7, Communications on Hydraulics, Department of Civil Engineering, Delft University of Technology.

Gold, I., 2010. LIDAR Quality Control Report Project PM_0901: Survey for Polygon P_6802, Environmental Agency, UK.

Gresswell, R.K., 1953. Sandy Shores in South Lancashire, Liverpool University Press, Liverpool.

Halcrow, 2009. North West England and North Wales Shoreline Management Plan 2, Appendix C: Baseline Processes, 40 pp (http://mycoastline.org/documents/AppendixC-C.4F_Seftoncoast.pdf).

Hallermeier, R.J., 1983. Sand Transport Limits in Coastal Structure Design, Proceedings, Coastal Structures '83, American Society of Civil Engineers, pp 703 – 716.

Harley, M.D. and Ciavola, P., 2013. Managing local coastal inundation risk using real-time forecasts and artificial dune placements, Coastal Engineering 77, 77 – 90.

Harley, M.D., Armaroli, C., Ciavola, P., 2011. Evaluation of XBeach predictions for a real-time warning system in Emilia-Romagna, Northern Italy. Journal of Coastal Research, Special Issue 64, 1861 – 1865.

Horsburgh, K.J., Wilson, C., 2007. Tide-surge interaction and its role in the distribution of surge residuals in the North Sea, Journal of Geophysical Research, Vol. 112, C08003, doi: 10.1029/2006JC004033.

Houston, J., 2010. The development of Integrated Coastal Zone Management (ICZM) in the UK: the experience of the Sefton Coast, Sefton's Dynamic Coast, Proceeding of the conference on coastal and geomorphology, biogeography and management, 289 – 305.

Jones, J.E., Davies, A.M., 1998. Storm surge computations for the Irish Sea using a three-dimensional numerical modelling including wave-current interaction, Continental Shelf Research 18, 201 – 251.

Karunarathna, H., Pender, D., Ranasinghe, R., Short, A.D., Reeve, D.E., 2014. The effects of storm clustering on beach profile variability, Marine Geology 348, 103 – 112.

Larson, M., Kraus, N., 1989. SBEACH: numerical model for simulating storm-induced beach change. Report 1: Empirical Foundation and Model Development, Technical Report, CERC-89-9. US Army Engineer Waterways Experiment Station, Vicksburg, MS. 267 pp.

Larson, M., Wise, R.A., Kraus, N., 2004.Modelling dune response by overwash transport. In: Mckee Smith, J. (Ed), Coastal Engineering 29th International Conference, World Scientific, Lisbon, Portugal, pp. 2133 – 2145.

Lesser, G., Roelvink, J.A., Van Kester, J.A.T.M., Stelling, G.S., 2004. Development and validation of a three dimensional morphological model, Coastal Engineering 51, 883 – 915.

Lindemer, C., Plant, N., Puleo, J., Thompson, D., Wamsley, T., 2010. Numerical simulation of a low-lying barrier island's morphological response to Hurricane Katrina, Coastal Engineering 57 (11), 985 – 995.

McAleavy, D., 2010. Sefton Beach Management – Twenty Years of Progress, Sefton's Dynamic Coast, Proceeding of the conference on coastal and geomorphology, biogeography and management, 318 – 326.

McCall, R., Van Thiel de Vries, J., Plant, N., Van Dongeren, A., Roelvink, J., Thompson, D., Reniers, A., 2010. Two-dimensional time dependent hurricane overwash and erosion modelling at Santa Rosa Island, Coastal Engineeirng 57 (7), 668 – 683.

Palmer, M.R., 2010. The modification of current ellipses by stratification in the Liverpool Bay ROFI, Ocean Dynamics 60, 219 – 226. doi 10.1007/s10236-009-0246-x

Palmsten, M., Holman, R., 2012. Laboratory investigation of dune erosion using stereo video, Coastal Engineering 60, 123 – 135.

Parker, W.R., 1969. A Report on Research Conducted into Aspects of the Marine Environment Affecting Coast Erosion between Ainsdale and Hightown, Lancashire, Lancashire County Council, pp 99.

Pender, D., Karunarathna, H., 2013. A statistical-process based approach for modelling beach profile variability, Coastal Engineering 81, 19 – 29.

Plater, A.J., Grenville, J., 2010. Liverpool Bay: linking the eastern Irish Sea to the Sefton Coast, Sefton's Dynamic Coast, Proceeding of the conference on coastal and geomorphology, biogeography and management, 41 – 43.

Pye, K., Blott, S.J., 2010. Geomorphology of Sefton Coast and dunes, Sefton's Dynamic Coast, Proceeding of the conference on coastal and geomorphology, biogeography and management, 131 – 159.

Pye, K., Blott, S.J., 2008. Decadal-scale variation in dune erosion and accretion rates: an investigation of the significance of changing storm tide frequency and magnitude on the Sefton Coast, UK. Geomorphology 102, 652 – 666.

1397 Pye, K., Neal, A., 1994. Coastal dune erosion at Formby Point, north Merseyside, England: causes and
1398 mechanisms. Marine Geology 119, 39 – 56.
1399
1400 Pye, K., Smith, A.J., 1988. Beach and dune erosion on the Sefton Coast, Northwest England, Journal of
1401 Coastal Research, SI. 3, 33 – 36.
1402
1403 Pugh, D.T., 1987. Tides, Surges and mean sea level rise: a hand book for engineers and scientists (472).
1404 Chichester: Wiley.
1405
1406 Ranasinghe, R., Callaghan, D., Stive, M.J.F., 2011. Estimating coastal recession due to sea level rise:
1407 beyond the Bruun rule, Climatic Change, DOI 10.1007/s10584-011-0107-8.
1408
1409 Roelvink, J.A., 2006. Coastal morphodynamic evolution techniques, Coastal Engineering 53, 277 – 287.
1410
1411 Roelvink, D., Reniers, A., van Dongeren, A., Van Thiel de Vries, J., McCall, R., Lescinski, J., 2009.
1412 Modelling storm impacts on beaches, dunes and barrier islands. Coastal Engineering 56, 1133 – 1152.
1413
1414 Roelvink, J., Stive, M.J.F., 1989. Bar-generating cross-shore flow mechanisms on a beach. Journal of
1415 Geophysical Research 94 (C4), 4785 – 4800.
1416
1417 Smith, P.H., 2010. Dragonflies (Odonata), Proceeding of the conference on coastal and geomorphology,
1418 biogeography and management, 175 – 177.
1419
1420 Soulsby, R., 1997. Dynamics of marine sands. Thomas Telford Publications, London, ISBN 0 7277 2584
1421 X.
1422
1423 Sallenger, A., 2000. Storm impact scale for barrier islands. Journal of Coastal Research 16 (3), 890 – 895.
1424

Souza, A.J., Brown, J.M., Williams, J.J., Lymbery, G., 2013. Application of an operational storm coastal impact forecasting system, Journal of Operational Oceanography, Vol. 6, 23 – 26.

Splinter, K.D., Palmsten, M.L., 2012.Modelling dune response to an East Coast Low. Marine Geology 329 – 331, 46 – 57.

Stive, M.J.F., Wind, H.G., 1986. Cross-shore mean flow in the surfzone. Coastal Engineering 10, 325 – 340.

Thomas, C.G., Spearman, J.R., Turnball, M.J., 2001. Historical morphological change in the Mersey Estuary. Continental Shelf Research, 22: 1775-1794.

Van Rijn, L. C., Walstra, D.J.R., Grasmeijer, B., Sutherland, J., Pan, S., Sierra, J.P., 2003. The predictability of cross-shore evolution of sandy beaches at the scale of storm and seasons using process-based profile models. *Coastal Engineering* 47, 295-327.

Van Thiel de Vries, J.S.M., Van Gent, M.R.A., Walstra, D.J.R., Reniers, A.J.H.M., 2008. Analysis of dune erosion processes in large-scale flume experiments, Coastal Engineering 55 (12), 1028 – 1040.

Vellinga, P., 1986. Beach and dune erosion during storm surges. Delft University of Technology, PhD Thesis.

White, S., 2010. The Birds of the Sefton Coast: A review, Proceeding of the conference on coastal and geomorphology, biogeography and management, 162 – 173.

Williams, J.J., Brown, J., Esteves, L.S., Souza, A., 2011. MICORE WP4 Modelling coastal erosion and flooding along the Sefton Coast NW UK, Final Report (http://www.micore.eu).

Wolf, J., 1981. Surge-tide interaction in the North Sea and River Thames, in Floods due to High Winds and Tides, edited by D.H. Peregrine, pp. 75 – 94, Elsevier, New York.

Wolf, J., Brown, J.M., Howarth, M.J., 2011. The wave climate of Liverpool Bay – observations and modelling, Ocean Dynamics 61, 639 – 655.

Wolf, J., Woolf, D.K., 2006. Waves and climate change in the north-east Atlantic. Geophysical Research Letter 33:L06604, doi: 1029/2005GL025113.

Woodworth, P.L., Flather, R.A., Williams, J.A.,Wakelin, S.L., Jevrejeva, S., 2007. The dependence of UK extreme sea levels and storm surges on the North Atlantic Oscillation, Continental Shelf Research 27 (7), 935 – 946.